INL/EXT-17-43189
Revision 0

AGR-5/6/7 Irradiation Test Predictions using PARFUME

William F. Skerjanc

September 2017

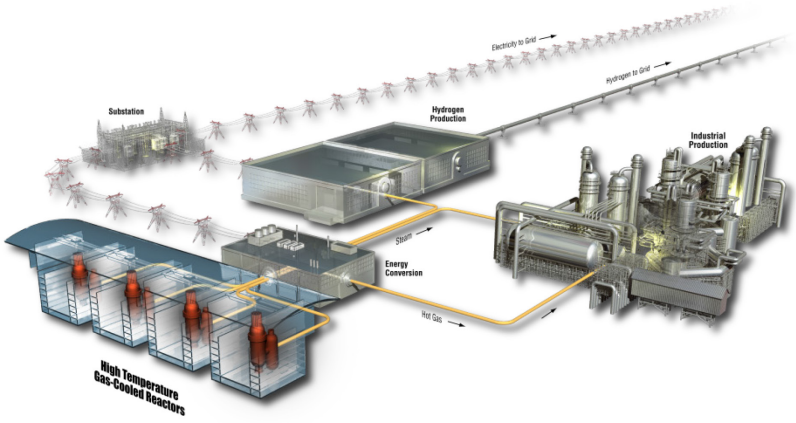

The INL is a
U.S. Department of Energy
National Laboratory
operated by
Battelle Energy Alliance

Idaho National Laboratory

INL/EXT-17-43189
Revision 0

AGR-5/6/7 Irradiation Test Predictions using PARFUME

William F. Skerjanc

September 2017

Idaho National Laboratory
INL ART TDO Program
Idaho Falls, Idaho 83415

http://www.inl.gov

Prepared for the
U.S. Department of Energy
Office of Nuclear Energy
Under DOE Idaho Operations Office
Contract DE-AC07-05ID14517

INL ART TDO Program

AGR-5/6/7 Irradiation Test Predictions using PARFUME

INL/EXT-17-43189
Revision 0

September 2017

Author:

William F. Skerjanc — 9/13/2017 Date

Technical Reviewer: (Confirmation of mathematical accuracy, and correctness of data and appropriateness of assumptions.)

Blaise P. Collin
Technical Reviewer — 9/13/2017 Date

Approved by:

Paul A. Demkowicz
AGR Fuels Director — 9/13/17 Date

Michelle T. Sharp
INL Quality Engineer — 9/13/17 Date

ABSTRACT

The PARticle FUel ModEl (PARFUME), a fuel performance modeling code used for high-temperature gas-cooled reactors, was used to model the Advanced Gas Reactor (AGR)-5/6/7 irradiation test using predicted physics and thermal data. The AGR-5/6/7 test consists of the combined fifth, sixth, and seventh planned irradiations of the AGR Fuel Development and Qualification Program. The AGR-5/6/7 test train is a multi-capsule, instrumented experiment that is designed for irradiation in the 133.4-mm diameter northeast flux trap position of the Advanced Test Reactor (ATR) at Idaho National Laboratory. Each capsule contains compacts filled with uranium oxycarbide unaltered fuel particles. This report documents the calculations performed to predict the failure probability of tristructural isotropic (TRISO)-coated fuel particles during the AGR-5/6/7 experiment. In addition, this report documents the calculated source term from the fuel. The calculations include modeling of the AGR-5/6/7 irradiation that is scheduled to occur from December 2017 to January 2021 over 13 ATR cycles, including nine normal cycles and four power axial locator mechanism cycles, for a total between 500 to 550 effective full power days.

The irradiation conditions and material properties of the AGR-5/6/7 test predicted zero fuel particle failures in Capsules 1, 2, and 4. Fuel particle failures were predicted in Capsule 3 due to internal particle pressure. These failures were predicted in the highest temperature compacts. Capsule 5 fuel particle failures were due to the inner pyrolytic carbon (IPyC) cracking causing localized stress concentrations in the silicon carbide layer. This capsule predicted the highest particle failures due to the lower irradiation temperature. In addition, shrinkage of the buffer and IPyC layer during irradiation resulted in formation of a buffer-IPyC gap. The two capsules at the two ends of the test train, Capsules 1 and 5, experienced the smallest buffer-IPyC gap formation due to the lower irradiation fluences and temperatures. Capsule 3 experienced the largest buffer-IPyC gap formation of 23.9 μm.

The release fraction of fission products silver (Ag), cesium (Cs), and strontium (Sr) vary depending on capsule location and irradiation temperature. The maximum release fraction of Ag occurs in Capsule 3, reaching up to 84.8% for the TRISO fuel particles. The release fraction of the other two fission products, Cs and Sr, are much smaller and, in most cases, less than 1%. The notable exception is again in Capsule 3, where the release fractions for Cs and Sr reach up to 9.7 and 19.1%, respectively.

CONTENTS

FIGURES

TABLES

ACRONYMS

AGR	Advanced Gas Reactor
AGR-5/6/7	Combined fifth/sixth/seventh irradiation test of the AGR Fuel Development and Qualification Program
ATR	Advanced Test Reactor
EFPD	effective full power day
FIMA	fissions per initial heavy metal atom
IPyC	inner pyrolytic carbon
NEFT	northeast flux trap
OPyC	outer pyrolytic carbon
PARFUME	PARticle FUel ModEl
PIE	post-irradiation examination
PyC	pyrolytic carbon
R/B	release to birth
SiC	silicon carbide
TAVA	time-average volume-average
TRISO	tristructural isotropic
UCO	uranium oxycarbide

AGR-5/6/7 Irradiation Test Predictions using PARFUME

1. INTRODUCTION

Several fuel and material irradiation experiments have been planned for the United States Department of Energy Advanced Gas Reactor (AGR) Fuel Development and Qualification Program. These experiments support development and qualification of tristructural isotropic (TRISO)-coated particle fuel for use in high-temperature gas-cooled reactors. The goals of these experiments are to provide irradiation performance data to support fuel process development, qualify fuel for normal operating conditions, support development and validation of fuel performance and fission product transport models and codes, and provide irradiated fuel and materials for post-irradiation examination (PIE) and safety testing (INL 2017). AGR-5/6/7 combined the fifth, sixth, and seventh in this series of planned experiments to test TRISO-coated, low-enriched uranium oxycarbide (UCO) fuel.

AGR-5/6/7 is planned for 500 to 550 effective full power days (EFPDs) or approximately two and a half calendar years. Final burnup values on a per compact basis will be greater than 6% fissions per initial heavy metal atom (FIMA) with at least one compact greater than 18% FIMA (Sterbentz 2017). Fast fluence ($E_n > 0.18$ MeV) values will range between 1.5 and 7.5×10^{25} n/m^2 with at last one compact in each test reaching a fast fluence greater than 5.0×10^{25} n/m^2. Time-average volume-average (TAVA) fuel temperatures on a capsule basis at the end of irradiation will range from 696°C in Capsule 5 to 1420°C in Capsule 3 (Murray 2017).

This report documents the calculations performed to predict the failure probability of TRISO-coated fuel particles during the AGR-5/6/7 experiment. In addition, this report documents the calculated source term from the fuel. The calculations include modeling of the AGR-5/6/7 irradiation that is scheduled to occur from December 2017 to January 2021 in the Advanced Test Reactor (ATR) (at Idaho National Laboratory) over 13 ATR cycles, including nine normal cycles and four power axial locator mechanism cycles, for a total between 500 to 550 EFPDs.

The modeling was performed using the PARticle FUel ModEl (PARFUME) computer code developed at Idaho National Laboratory. PARFUME is an advanced gas-cooled reactor fuel performance modeling and analysis code (Miller et al. 2009). It has been developed as an integrated mechanistic code that evaluates the thermal, mechanical, and physico-chemical behavior of fuel particles during irradiation to determine the failure probability of a population of fuel particles. It factors the particle-to-particle statistical variations in physical dimensions and the material properties that arise from the fuel fabrication process, accounting for most viable mechanisms that can lead to particle failure. The code also determines the diffusion of fission products from the fuel through the particle coating layers and through the fuel matrix to the coolant boundary. The subsequent release of fission products is calculated at the compact level (i.e., release of fission products from the compact). PARFUME calculates the release fraction as a ratio of the number of atoms released from the compact to the amount produced in the compact fuel kernels and through uranium contamination.

Calculations were performed with PARFUME Version 2.23 (as configured by the Revision Control System) compiled with Intel FORTRAN Compiler 11.1.073 on a SGI ICE X platform operating under SUSE Linux Enterprise Server 11. PARFUME was executed with its fast integration scheme to calculate the particle failure probabilities and with its Monte Carlo scheme to obtain the fractional releases of fission products. In addition, this study was conducted in accordance to quality standard NQA-1-2008/-1a-2009, “Quality Assurance Requirements for Nuclear Facility Applications” (ASME 2008).

Details associated with completing these calculations are provided in the remainder of this report. The AGR-5/6/7 irradiation experiment description is briefly introduced in Section 2, PARFUME modeling is outlined in Section 3, results are described in Section 4, conclusions are given in Section 5, and references are listed in Section 6.

2. AGR-5/6/7 IRRADIATION EXPERIMENT

As defined in the technical program plan for the AGR Fuel Development and Qualification Program (INL 2017), the objectives of the AGR-5/6/7 experiment are as follows:

1. Irradiate reference design fuel containing low-enriched UCO TRISO fuel particles to support fuel qualification.
2. Establish the operating margins for the fuel beyond normal operating conditions.
3. Provide irradiated fuel performance data and irradiate fuel samples for PIE and safety testing.

To achieve the test objectives outlined above, in accordance with requirements from the technical program plan the AGR Fuel Development and Qualification Program (INL 2017) and the Irradiation Test Specification (Maki 2015), AGR-5/6/7 will be irradiated in the northeast flux trap (NEFT) position of ATR. A cross-sectional view of the ATR core, which indicates the NEFT location, is displayed in Figure 1.

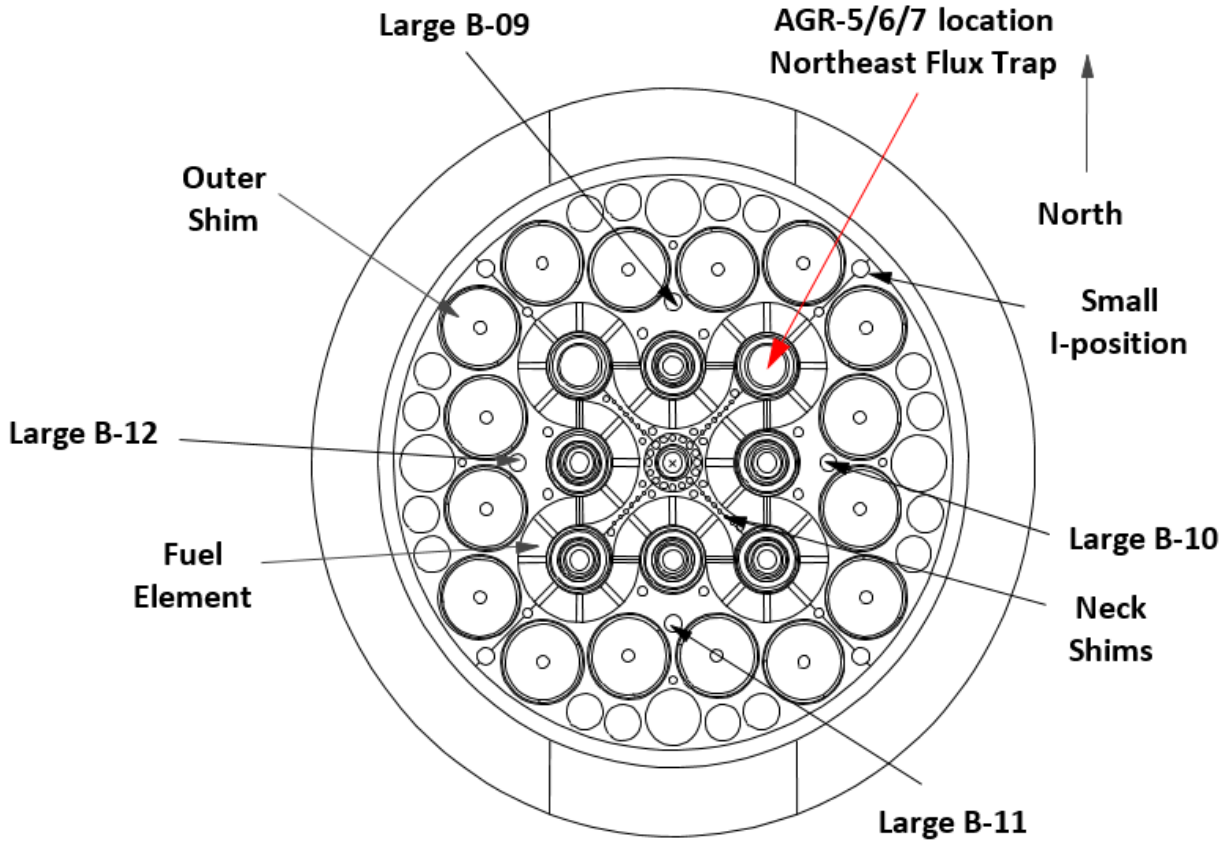

Figure 1. ATR core cross section displaying the NEFT position.

The AGR-5/6/7 test train is a multi-capsule, instrumented experiment that is designed for irradiation in the 133.4-mm diameter NEFT position of ATR. Figure 2 illustrates the axial schematic of the AGR-5/6/7 test train containing four AGR-5/6 capsules (Capsules 1, 2, 4, and 5) and the AGR-7 capsule (Capsule 3). Figure 3 illustrates the radial view of the capsules.

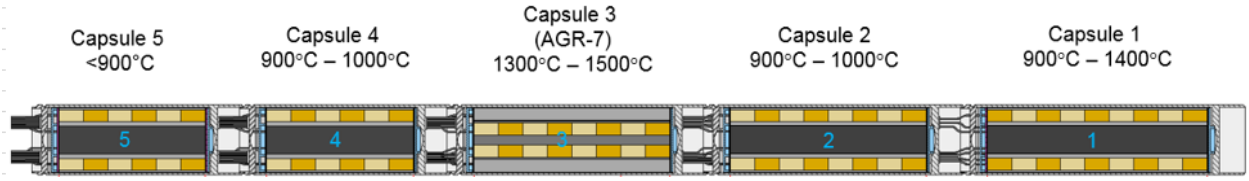

Figure 2. Axial schematic of the AGR-5/6/7 test train.

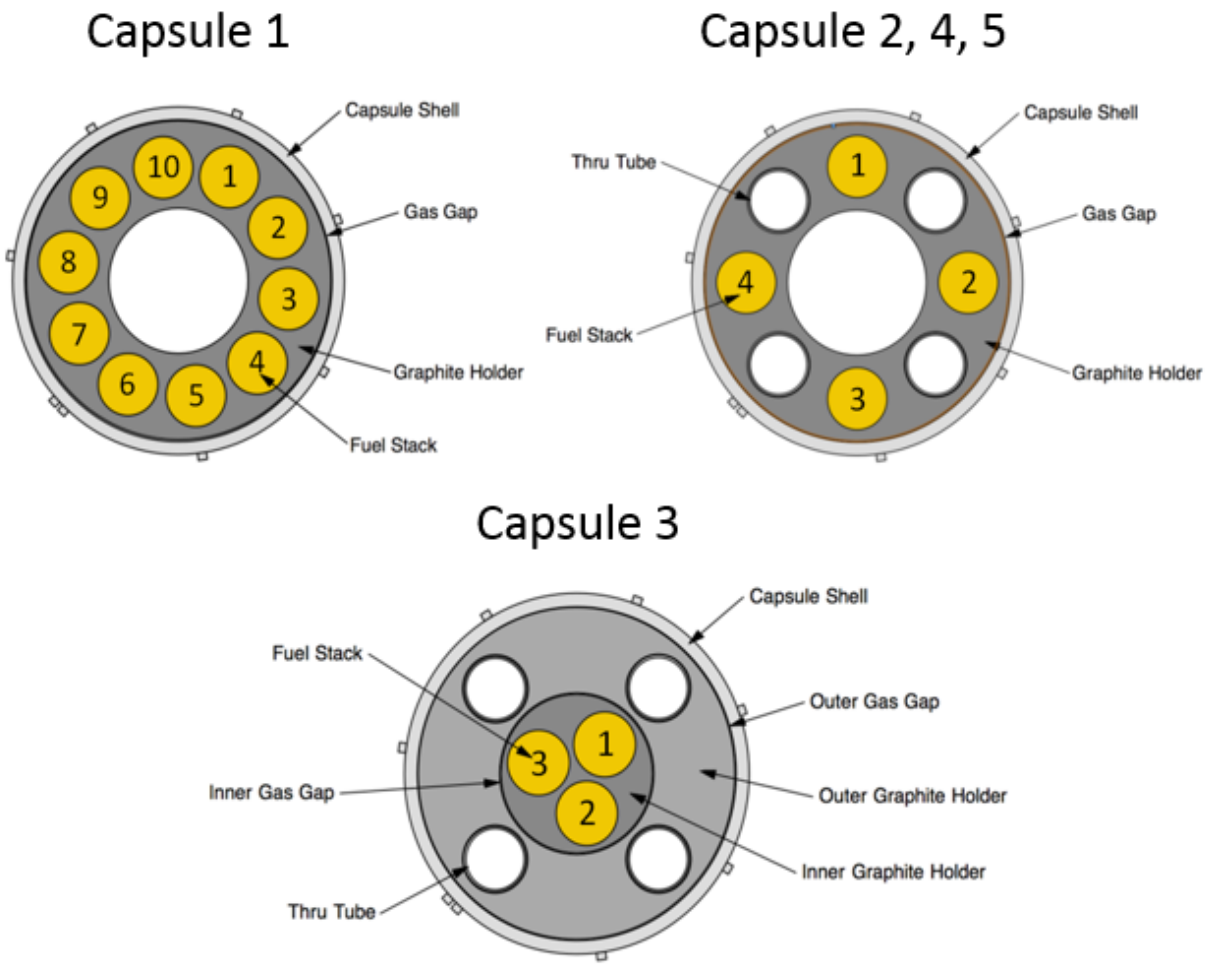

Figure 3. Cross sections of the AGR-5/6/7 capsules showing the compact stacks.

For AGR-5/6, 30% of the ~520,000 particles will operate at less than 900°C, 30% will operate at 900 to 1050°C, 30% will operate at 1050 to 1250°C, and the remaining 10% will operate at 1250 to 1350°C. For the margin test, AGR-7, all ~55,000 particles will operate at 1350 to 1500°C. The burnup and fast neutron fluence specifications are identical for the AGR-5/6 and AGR-7 tests. In each test, compact average fuel burnup will be greater than 6% for all compacts and greater than 18% FIMA for at

least one compact. The fuel will experience fast neutron fluences between approximately 1.5 and 7.5×10^{25} n/m^2 (E > 0.18 MeV) and at least one compact in each test will experience a fast neutron fluence greater than 5.0×10^{25} n/m^2 (E > 0.18 MeV). To attain these goals and still be able to control the temperature in the capsules, two packing fractions of compacts are used in the test train. Compacts with a 40% nominal packing fraction are used in Capsules 1 and 5, and compacts with a 25% nominal packing fraction are used in Capsules 2, 3, and 4.

Fuel for AGR-5/6/7 contains reference design UCO TRISO-coated particles that are slightly less than 1 mm in diameter. Each particle has a central reference kernel that contains fuel material, a porous carbon buffer layer, an inner pyrolytic carbon (IPyC) layer, a silicon carbide (SiC) barrier coating, and an outer pyrolytic carbon (OPyC) layer as depicted in Figure 4 with each layers functions described in Table 1. Kernels for AGR-5/6/7 consist of low-enriched UCO fuel.

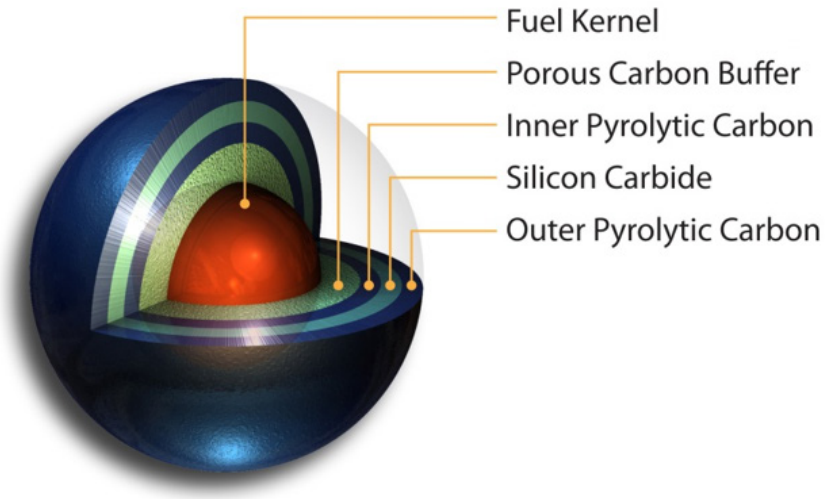

Figure 4. Typical TRISO-coated fuel particle.

Table 1. Primary functions of particle fuel components.

Component	Primary Function
Kernel	Contains fissile/fertile fuel
Buffer	Provides void space for fission product gases and accommodates differential changes in dimensions between coating layers and kernel
IPyC	Structural layer and fission gas barrier that protects the kernel during SiC deposition and the SiC layer from most fission products during irradiation
SiC	Primary structural layer and primary fission product barrier
OPyC	Structural layer that also permits embedding the particles in graphitic matrix material

A complete description of the fuel kernels, particles, compacts, and physics and thermal analyses is presented in the AGR-5/6/7 test plan (Collin 2017).

3. PARFUME MODELING

PARFUME was used to model the AGR-5/6/7 experiment to determine the probability of fuel particle failure and the release fractions of the fission products silver (Ag), cesium (Cs), and strontium (Sr) to determine the source term. The analysis considered conventional fuel particle failure (i.e., typical pressure vessel failure) and multidimensional failure mechanisms (i.e., IPyC cracking, asphericity, and debonding). The source terms were calculated assuming no fuel particle failures at time equal to zero. Key aspects of the PARFUME modeling of these AGR-5/6/7 conditions are described in the following subsections.

3.1 Boundary/Irradiation Conditions

PARFUME is designed to evaluate fuel performance based on user inputs for neutron fluence and burnup, with a corresponding set of thermal conditions. Results from neutronics analyses and/or measured values are possible sources for fluence and burnup inputs. For this analysis, compact-specific fluence and burnup results from neutronics (Sterbentz 2017) and thermal (Murray 2017) analyses performed as part of the AGR-5/6/7 design report were used. It was determined that AGR-5/6/7 would have 194 compacts (Collin 2017) and a subset was chosen for this study by coupling minimum and maximum values and adding compact averages to create an envelope of possible irradiation conditions. All data is shown in Table 2.

PARFUME has considerable flexibility relative to the application of thermal conditions affecting fuel particles. A user may define the thermal conditions for the outer surfaces of the fuel-bearing materials (e.g., the outer surface of a pebble in the case of a pebble bed reactor or the coolant channel surface of a unit cell containing fuel compacts in the case of a prismatic reactor) or the user may define fuel-bearing material temperatures directly. Options for the outer surfaces of the fuel-bearing materials include defining either a time-dependent set of temperatures or a time-dependent set of heat transfer coefficients, with a corresponding time-dependent set of sink temperatures. Fuel-bearing material temperatures can be defined directly as time-dependent values that are applicable to the entire material or the user may divide the material into regions and supply time-dependent temperatures for each region. The direct specification of fuel-bearing material temperatures was applied here.

For the purpose of calculating the fuel failure, calculations were made assuming that each compact in the five capsules followed a TAVA temperature throughout the entire irradiation.

The modeling of fission product release was made on a compact basis; therefore, its results could be used as a source term to support the PIE effort on fission product transport. Since these calculations serve as only a prediction, the TAVA temperatures were used to be consistent with the failure probability analysis. A more thorough analysis can be completed post-irradiation using the actual daily temperatures to produce a more accurate source term. In addition, the failure fractions of the IPyC, SiC, and OPyC directly impact the diffusion of fission products through the particle. When one of these layers fail, the diffusivity is reduced essentially opening up that layer for free migration through that layer.

Table 2. Compact thermal conditions and end-of-irradiation burnup and fluence.

Capsule	Compact	Fluence ($\times 10^{25}$ n/m^2)	Burnup (%FIMA)	TAVA (°C)	Notes
1	1-1-1	2.21	7.42	888	Low fast fluence, minimum TAVA
	1-8-6	5.74	13.96	1241	Maximum TAVA
	1-9-6	5.95	14.47	1146	Maximum fast fluence
	Average	4.32	11.49	1105	Average fast fluence, burnup, and TAVA
2	2-1-1	6.13	16.71	851	Low fast fluence, minimum TAVA
	2-7-3	7.21	18.58	935	Maximum TAVA

Capsule	Compact	Fluence ($\times 10^{25}$ n/m^2)	Burnup (%FIMA)	TAVA (°C)	Notes
	2-8-3	7.24	18.56	923	Maximum fast fluence
	Average	6.77	17.97	910	Average fast fluence , burnup, and TAVA
3	3-1-1	7.13	17.70	1292	Low fast fluence, minimum TAVA
	3-3-2	7.35	18.33	1405	Maximum fast fluence
	3-6-2	7.18	18.19	1421	Maximum TAVA
	Average	7.17	18.03	1382	Average fast fluence, burnup, and TAVA
4	4-1-3	6.61	17.44	913	Maximum fast fluence
	4-4-4	6.07	16.77	933	Maximum TAVA
	4-6-2	5.31	15.47	881	Low fast fluence, minimum TAVA
	Average	6.01	16.63	916	Average fast fluence, burnup, and TAVA
5	5-1-3	4.54	12.67	803	Maximum fast fluence
	5-2-3	4.19	12.17	812	Maximum TAVA
	5-6-1	2.25	8.24	696	Low fast fluence, minimum TAVA
	Average	3.45	10.74	777	Average fast fluence, burnup, and TAVA

3.2 Input Parameters

PARFUME input parameters for modeling the AGR-5/6/7 experiment were taken from the fuel product specification (Marshall 2017). The fuel particle geometry and material properties are listed in Table 3 and Table 4, respectively.

The Abaqus calculations were made using an asphericity of 1.04 that corresponds to the sphericity at the OPyC level. There was no measurement of the sphericity at the SiC level, which is the determining factor for asphericity calculations. Therefore, the calculations overestimated the asphericity in the Abaqus (and subsequent PARFUME) calculations.

Table 3. AGR-5/6/7 TRISO fuel particle geometry.

Attribute	Mean Value	Standard Deviation
Kernel diameter (μm)	425	10
Buffer thickness (μm)	100	15
IPyC thickness (μm)	40	4
SiC thickness (μm)	35	3
OPyC thickness (μm)	40	4
SiC aspect ratio	1.04	0.02

Table 4. AGR-5/6/7 TRISO fuel particle attributes.

Attribute	Mean Value	Standard Deviation
Kernel density	10.40 Mg/m^3	—
Buffer density	1.05 Mg/m^3	0.10 Mg/m^3
IPyC density	1.90 Mg/m^3	0.05 Mg/m^3
OPyC density	1.90 Mg/m^3	0.05 Mg/m^3

Table 4. (continued).

Attribute	Mean Value	Standard Deviation
IPyC Bacon anisotropy factor	1.045	0.005
OPyC Bacon anisotropy factor	1.035	0.005
Pyrolytic carbon Poisson's ratio in creep	0.5	—
U-235 enrichment	15.500 wt%	—
Oxygen-to-uranium	1.500 atom ratio	—
Carbon-to-uranium	0.400 atom ratio	—

3.3 Multidimensional Stress

In addition to the one-dimensional behavior of a symmetrical spherical fuel particle, PARFUME considers multidimensional behavior, including aspherical geometry, cracking of the IPyC layer, and partial debonding of the IPyC from the SiC. To model these effects, PARFUME uses the results of detailed finite element analyses for cracked, debonded, and/or aspherical particles in conjunction with results from the PARFUME, closed form, one-dimensional solution to make a statistical approximation of the stress levels in any particle (Miller et al. 2003; Miller et al. 2004). Abaqus Version 6.9-2 (Abaqus 2009) was used to perform the finite element stress analyses to capture the multidimensional effects of asphericity and IPyC cracking. It has been previously determined that variations in parameters that greatly impact the multidimensional results include the IPyC, SiC, and OPyC thicknesses for both IPyC cracking and asphericity (Skerjanc et al. 2016). In addition, the degree to which the fuel particle is aspherical also impacts the probability of SiC failure due to pressure. IPyC/SiC debonding was not considered in this analysis because current fuel manufacturing practices have greatly improved the IPyC/SiC bond strength (about 100 MPa), resulting in zero fuel particle failures due to debonding as calculated by PARFUME.

3.4 Material Properties

Material properties used in PARFUME are discussed in great detail in the *PARFUME Theory and Model Basis Report* (Miller et al. 2009). The elastic moduli and swelling strains for the IPyC and OPyC are treated as functions of fluence. The effective range for these properties extends to a fluence of 3.96×10^{25} n/m^2. However, an approximation was necessary to enable PARFUME modeling of some capsules in the AGR-5/6/7 test where the end-of-life fluence reaches as much as 7.35×10^{25} n/m^2. The approximation consists of treating the elastic moduli and swelling strain rates as constants in PARFUME beyond a fluence level of 3.96×10^{25} n/m^2 ($E_n > 0.18$ MeV).

The historical creep coefficient for the pyrocarbon layers (CEGA 1993) was found to be significantly lower than what has been used in other fuel performance models. It has also been found that PARFUME gives favorable comparisons with results of the New Production - Modular High Temperature Gas Reactor experiments if the historical creep coefficient is approximately doubled (Miller et al. 2003). Therefore, the creep coefficient used in predictions for the AGR-5/6/7 test was set equal to twice the historical value.

There is significant uncertainty in how well the physical properties of the coating layers are known. The accuracy of the failure probability predictions from any fuel performance code relies on the accuracy of these properties.

3.5 Physico-Chemical Behavior

The internal gas pressure is calculated in PARFUME as a function of time according to the Redlich-Kwong equation of state. Parameters utilized in this equation are derived from the critical temperature and pressure of each gas species occupying the void volume within the particle. PARFUME considers generation of carbon monoxide and release of the noble gas fission products (i.e., xenon and krypton) in this pressure calculation.

Carbon monoxide production can be calculated in PARFUME using an algorithm derived from thermochemical free energy minimization calculations performed by the HSC computer code. However, for this analysis, carbon monoxide production was not calculated since it is minimal in UCO fuel. PARFUME calculates fission product gas release caused by both recoil and diffusion. Direct fission recoil from the kernel to the buffer is accounted for by geometrical considerations and fission fragment ranges derived from compiled experimental data. Diffusive release is calculated according to the Booth equivalent sphere diffusion model, which utilizes an effective diffusion coefficient formulated by Turnbull. This effective diffusion coefficient accounts for intrinsic, thermal, and irradiation-enhanced diffusion.

A complete description of the treatment of the physico-chemical behavior can be found in the *PARFUME Theory and Model Basis Report* (Miller et al. 2009).

3.6 Failure Mechanisms Considered

Four potential failure mechanisms are currently considered in PARFUME. The first is a pressure vessel failure caused by buildup of gases (e.g., fission, carbon monoxide). Stresses for this failure mechanism are determined using the one-dimensional solution in PARFUME for a three-layer (IPyC-SiC-OPyC) particle. Because of asphericity in the particle shape, these stresses are modified based on the results of the finite element analysis of aspherical particles. Some particles' internal pressures were found to trigger this failure mechanism in AGR-5/6/7 test calculations.

The second mechanism considered is failure of the SiC layer caused by partial debonding of the IPyC from the SiC. Debonding, if it occurs, results from the IPyC shrinking inward away from the SiC during irradiation. PARFUME first determines whether debonding between the layers occurs by comparing the radial stress between layers with the bond strength between layers. If debonding is determined to occur, then the code estimates the stress in the SiC layer and accounts for the multidimensional effects using a previously documented methodology (Miller et al. 2004). Because AGR-5/6/7 particle fabrication was based on German processes, the bond strength was set at a value that is considered to be representative for German particles (i.e., 100 MPa). At this bond strength, IPyC/SiC debonding was not predicted; therefore, debonding did not contribute to particle failures in the AGR-5/6/7 test.

The third failure mechanism considered in PARFUME is migration of the fuel kernel into the SiC layer under the influence of a temperature gradient (or the amoeba effect). This effect is driven by the production of carbon monoxide and is only prominent with UO_2 kernels and is limited with UCO kernels. Therefore, the amoeba effect made no contribution to particle failures in these analyses.

The fourth and final failure mechanism currently considered in PARFUME is failure of the SiC layer caused by irradiation-induced shrinkage and the associated cracking of the IPyC layer. The presence of a crack in the IPyC layer creates a stress concentration in the SiC layer. To treat the multidimensional effects of this stress concentration, PARFUME estimates stresses in the SiC layer that result from the presence of a crack based on a previously documented methodology. In evaluating failures caused by IPyC cracking, PARFUME first determines whether the IPyC layer cracks using the Weibull statistical theory. If the IPyC layer is predicted to crack, the particle is evaluated for failure of the SiC layer due to the presence of the crack. Some fuel particle failures in AGR-5/6/7 test calculations were found to be caused by this mechanism.

Chemical attack of the SiC layer by palladium (Pd) represents another potential failure mechanism. Scoping calculations have shown that fuel particle failure occurs when penetration through the thickness of the SiC is complete, leading to the direct release of fission products.

PARFUME uses the Weibull statistical theory to determine whether particles fail, using a mean strength for the SiC layer based on a stress distribution corresponding to the failure mechanism under consideration. The failure modes are implemented such that a particle fails only in the mode of failure that would occur first for that particle. The code retains the time at which the failures occur, allowing for construction of a time evolution of the failure probability for a batch of fuel particles. Weibull parameters that are used to evaluate failures of the SiC layer and cracking of the IPyC layer are discussed in the CEGA report (CEGA 1993). Failure of the SiC layer in PARFUME is assumed to lead to full TRISO failure.

4. RESULTS

Results from the AGR-5/6/7 test predictions were obtained using PARFUME and are based on the inputs and modeling parameters discussed previously. These results include fuel particle failure probability, buffer-IPyC gap formation, and fission product release fractions. The results of particle failure probability were obtained using the fast (i.e., 2-loop) integration solver implemented in PARFUME as opposed to the full-loop integration or Monte Carlo method; this is due to the significant reduction in run times. It has been previously demonstrated that using the fast integration method does not adversely impact the accuracy of the results (Miller 2007). The fission product release calculations were run using the Monte Carlo scheme of PARFUME and the number of histories in these calculations were chosen to obtain the failure probabilities calculated by the integration scheme so that fission product release can take potential failures of the coating layers into account.

4.1 Fuel Particle Failure Probability

It is assumed that a fuel particle has failed when the SiC layer has become compromised and cracked, which leads to its inability to retain fission products. The primary mechanisms leading to SiC cracking and subsequent fuel particle failure in the AGR-5/6/7 analyses are due to IPyC cracking and pressure; it was determined that no fuel particle failure was predicted due to the amoeba effect or IPyC/SiC debonding. Complete results for the fuel particle failure probability analyses for the AGR-5/6/7 test are summarized in Table 5 and illustrated in Figure 5 through Figure 9. Assuming 3442 particles per compact, zero fuel particle failures per compact analyzed were predicted in Capsule 1. There were some particle failures in the compacts analyzed in Capsule 5. These SiC failures are due the lower temperature causing less creep to counteract the shrinkage causing the probability of IPyC cracking to increase (for compact 5-6-1, it was predicted that 85.5% of the particles would experience IPyC cracking). Assuming 2275 fuel particles per compact, zero fuel particle failures per compact analyzed were predicted in Capsules 2 and 4 while there were some particle failures in the compacts in Capsule 3. In general, the probability of fuel particle failures in Capsule 5 can be attributed to IPyC cracking and in Capsule 3 due to pressure. The primary driver of pressure-related failures is due to the production of fission gas coupled with the elevated temperatures. Compact 3-6-2, at the maximum temperature, experienced the largest Pd penetration into the SiC layer of 34.3 μm, which is less than the actual SiC layer thickness (35.0 μm). The SiC layer is considered failed at 100% penetration but it is not linked to any failure probability calculations in PARFUME.

Table 5. AGR-5/6/7 fuel particle failure probability results.

Capsule	Compact	Fluence ($\times 10^{25}$ n/m^2) [E > 0.18 MeV]	Burnup (%FIMA)	Temperature (°C)	Probability of Failure due to				Estimated Number of Particle Failures
					SiC Failure	IPyC Cracking	Pressure	IPyC Cracking	
1	1-1-1	2.21	7.42	888	5.0E-05	5.0E-05	0.0E+00	2.74E-01	0
	1-8-6	5.74	13.96	1241	1.4E-07	1.0E-08	1.3E-07	2.16E-03	0
	1-9-6	5.95	14.47	1146	9.7E-08	9.2E-08	4.8E-09	7.02E-03	0
	Average	4.32	11.49	1105	2.5E-07	2.5E-07	0.0E+00	1.20E-02	0
2	2-1-1	6.13	16.71	851	9.9E-05	9.9E-05	0.0E+00	4.06E-01	0
	2-7-3	7.21	18.58	935	1.7E-05	1.7E-05	0.0E+00	1.45E-01	0
	2-8-3	7.24	18.56	923	2.3E-05	2.3E-05	0.0E+00	1.71E-01	0
	Average	6.77	17.97	910	3.0E-05	3.0E-05	0.0E+00	2.04E-01	0
3	3-1-1	7.13	17.70	1292	2.5E-05	3.3E-09	2.5E-05	1.18E-03	0
	3-3-2	7.35	18.33	1405	3.2E-04	5.0E-10	3.2E-04	5.89E-04	1
	3-6-2	7.18	18.19	1421	3.7E-04	4.2E-10	3.7E-04	5.75E-04	1
	Average	7.17	18.03	1382	1.9E-04	6.7E-10	1.9E-04	6.04E-04	0
4	4-1-3	6.61	17.44	913	2.8E-05	2.8E-05	0.0E+00	1.97E-01	0
	4-4-4	6.07	16.77	933	1.8E-05	1.8E-05	0.0E+00	1.49E-01	0
	4-6-2	5.31	15.47	881	5.7E-05	5.7E-05	0.0E+00	2.95E-01	0
	Average	6.01	16.63	916	2.6E-05	2.6E-05	0.0E+00	1.89E-01	0
5	5-1-3	4.54	12.67	803	2.0E-04	2.0E-04	0.0E+00	5.98E-01	1
	5-2-3	4.19	12.17	812	1.8E-04	1.8E-04	0.0E+00	5.63E-01	1
	5-6-1	2.25	8.24	696	4.8E-04	4.8E-04	0.0E+00	8.55E-01	2
	Average	3.45	10.74	777	2.8E-04	2.8E-04	0.0E+00	6.88E-01	1

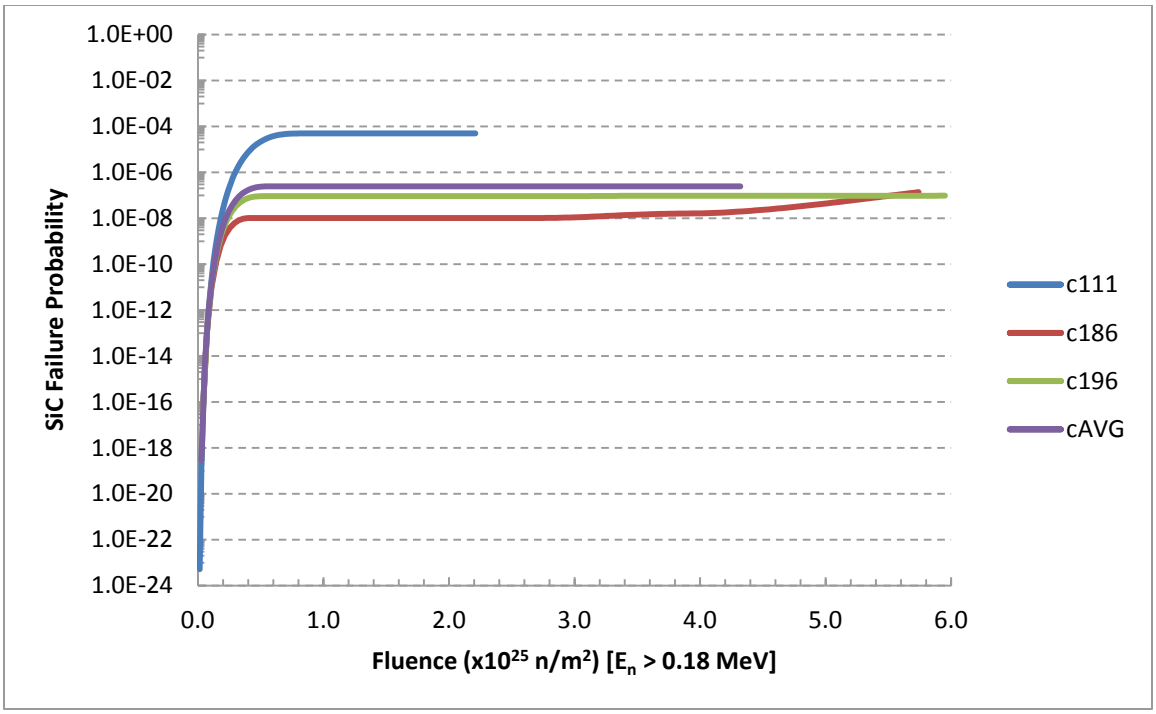

Figure 5. Capsule 1 fuel particle failure probability.

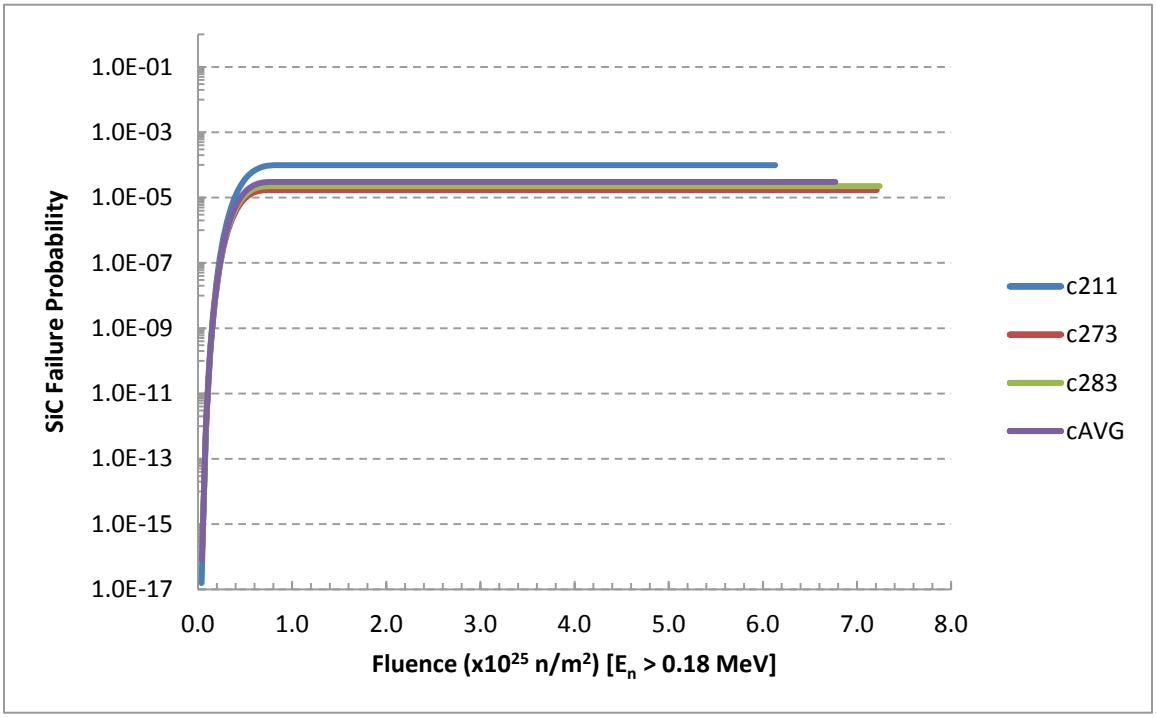

Figure 6. Capsule 2 fuel particle failure probability.

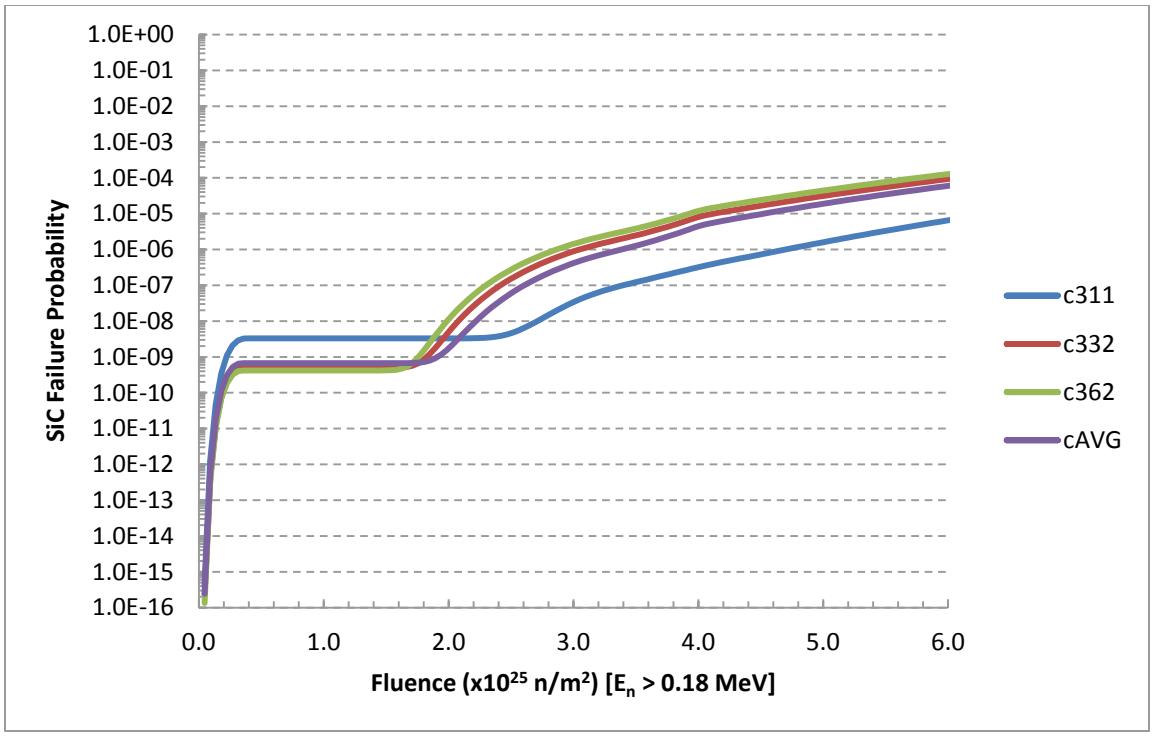

Figure 7. Capsule 3 fuel particle failure probability.

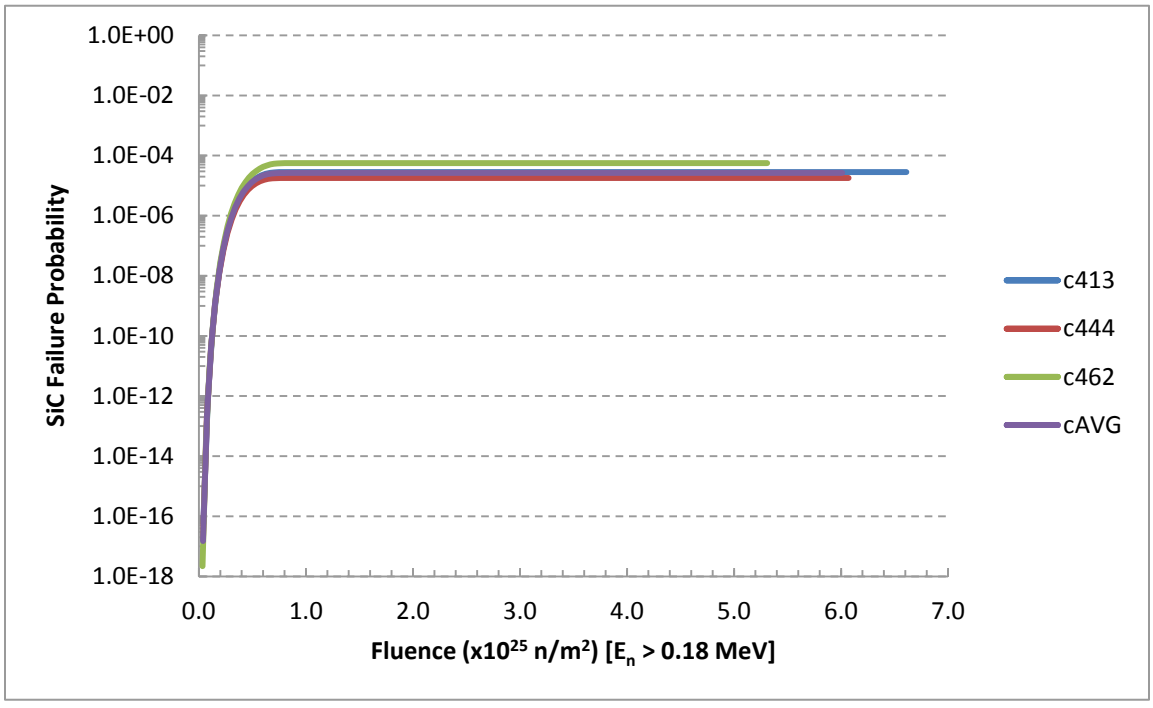

Figure 8. Capsule 4 fuel particle failure probability.

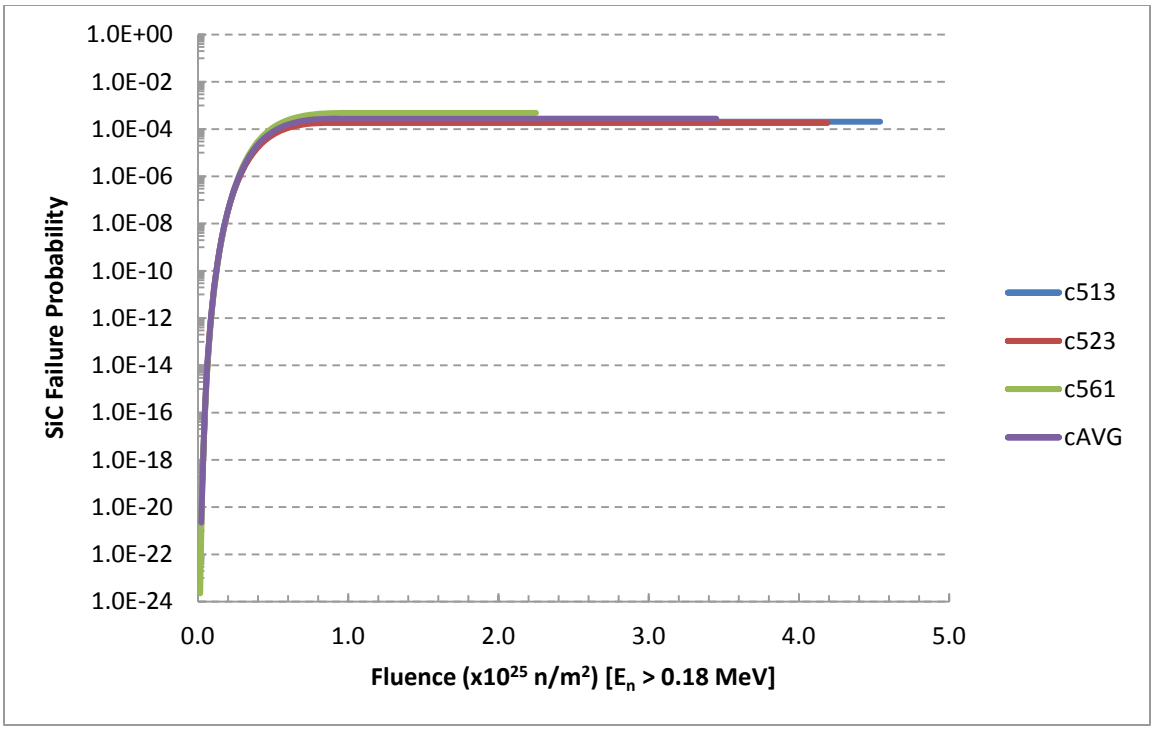

Figure 9. Capsule 5 fuel particle failure probability.

4.2 Buffer-IPyC Gap

Irradiation can lead to development of a gap between the buffer and IPyC layer. The gap can develop as a result of the combined effects of kernel swelling; shrinkage and creep in the buffer and IPyC layers; the effects of particle internal pressure, and the kernel/buffer contact pressure. However, differences in density between the buffer and the IPyC layer is a primary factor in the process. The buffer, which is much more porous than the dense IPyC layer, shrinks more during irradiation. The growth rate for the gap size slows as the buffer becomes denser during irradiation. PARFUME models the gap formation in 1-D geometry assuming the kernel/buffer remain concentrically centered inside the IPyC layer. The size of these gaps for the compacts selected are shown in Figure 10 through Figure 14 for nominal particles, assuming the outer surfaces of those particles follow capsule-specific volume-averaged temperatures. Inspection of these figures indicates that the gap width is closely correlated with fluence, which is correlated with the axial position of the capsules in the ATR core. Because ATR operates with a cosine-like profile, gap widths tend to be smallest in the outermost capsules (i.e., Capsules 1 and 5 that are exposed to relatively low fluence levels) and largest in the capsule at the core mid-plane (numbered 3 that is exposed to relatively high fluence levels).

The buffer-IPyC gap can be a significant fraction of the thermal resistance in a fuel particle. Consequently, if other conditions are equal, temperature differentials (i.e., from the kernel centerline to the outer surface of the OPyC) are higher across particles with larger gaps. This trend is apparent in Figure 15 through Figure 19, where temperature differentials are shown assuming the outer surfaces of particles follow volume-averaged temperatures. In these figures, temperature differentials are higher in center capsules' particles than in Capsules 1 and 5 particles, which would be expected given the capsule-to-capsule differences in the buffer-IPyC gaps (shown in Figure 10 through Figure 14).

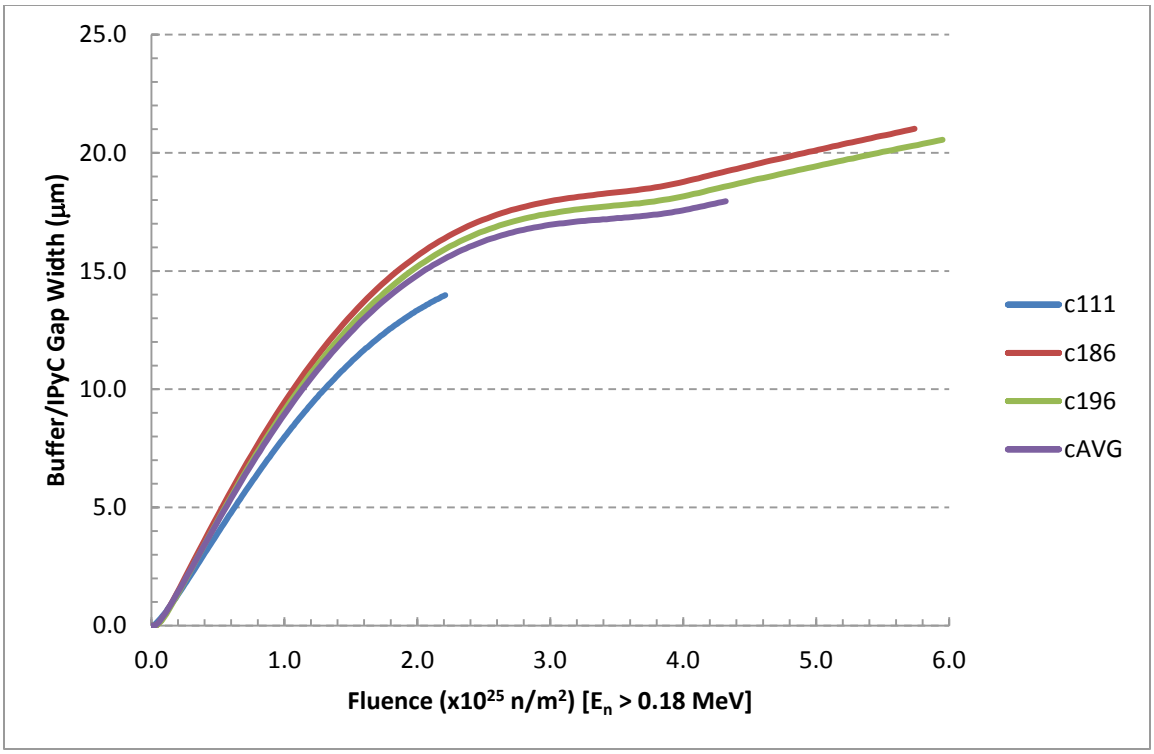

Figure 10. Capsule 1 buffer-IPyC gap width in nominal particles.

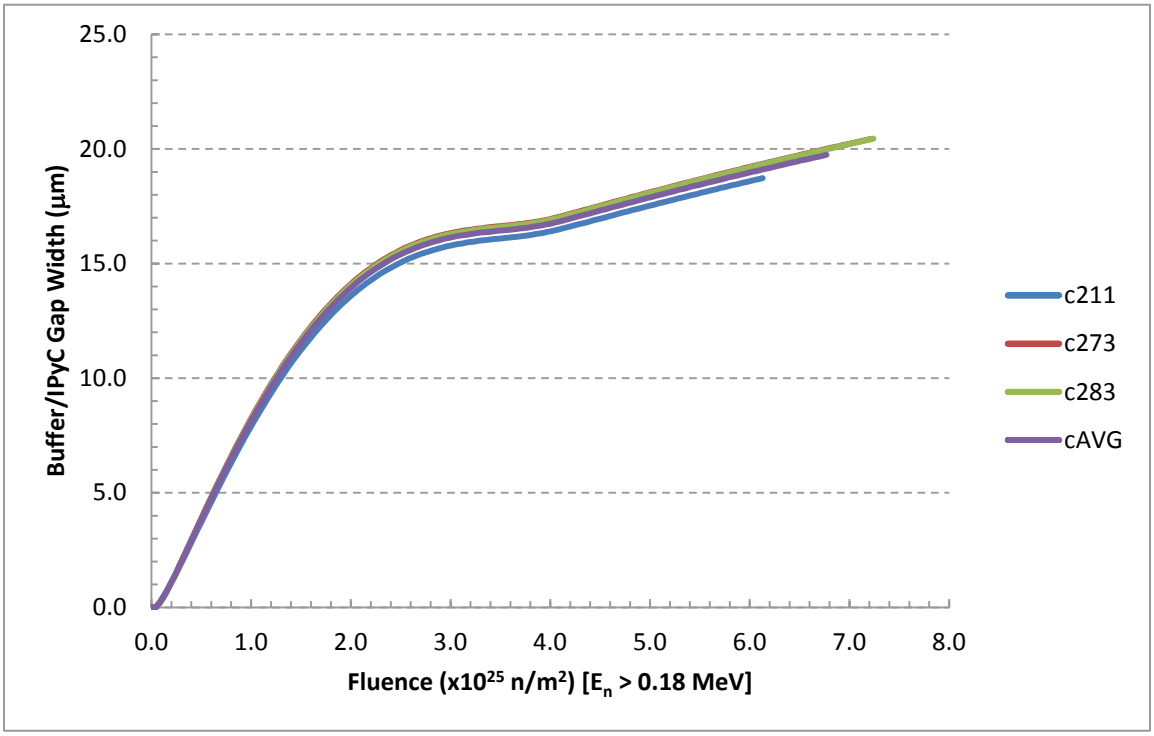

Figure 11. Capsule 2 buffer-IPyC gap width in nominal particles.

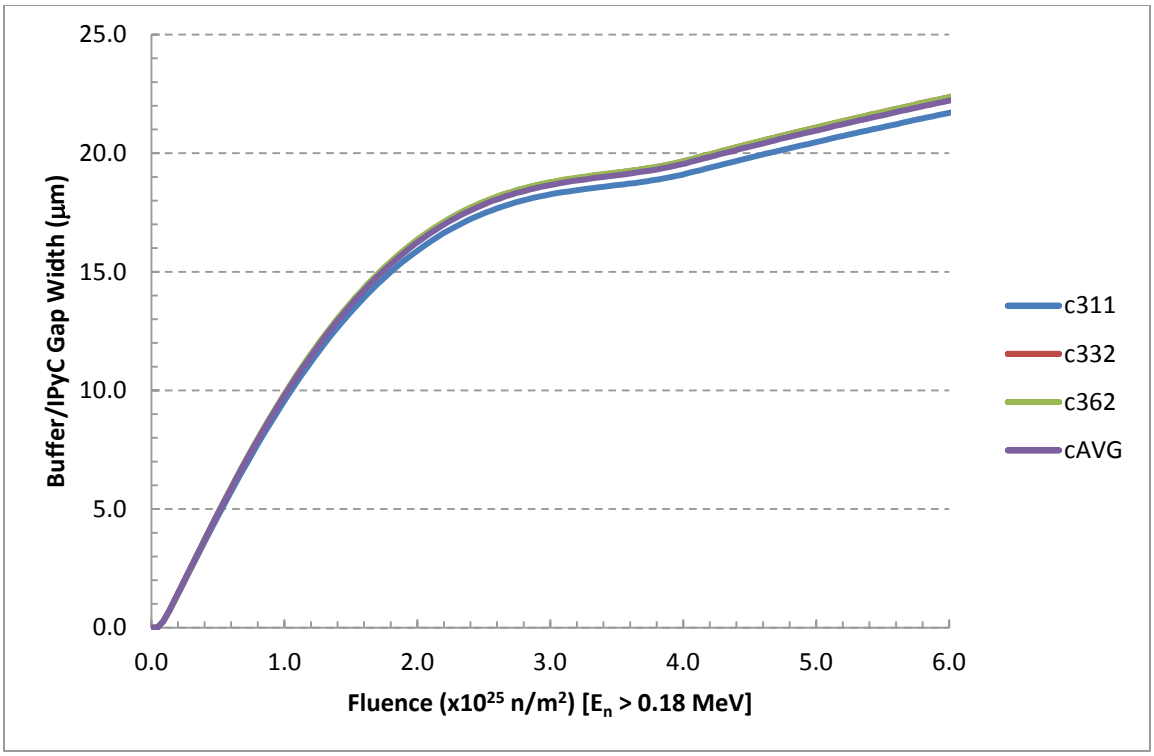

Figure 12. Capsule 3 buffer-IPyC gap width in nominal particles.

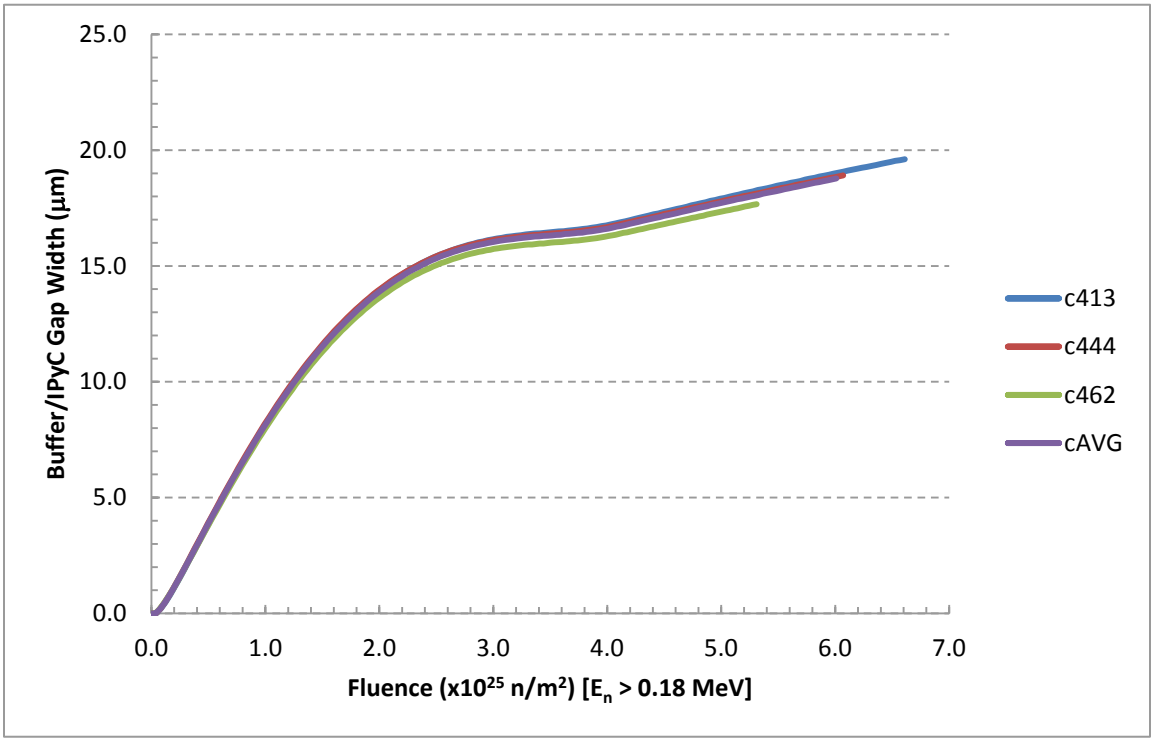

Figure 13. Capsule 4 buffer-IPyC gap width in nominal particles.

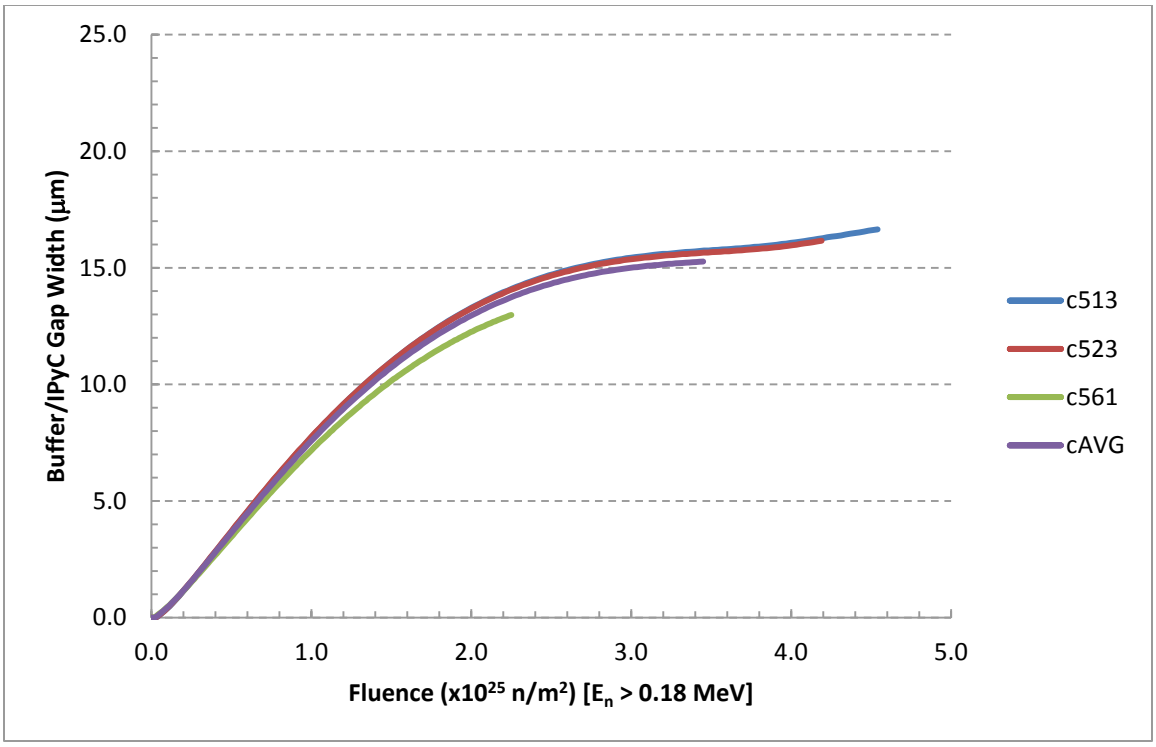

Figure 14. Capsule 5 buffer-IPyC gap width in nominal particles.

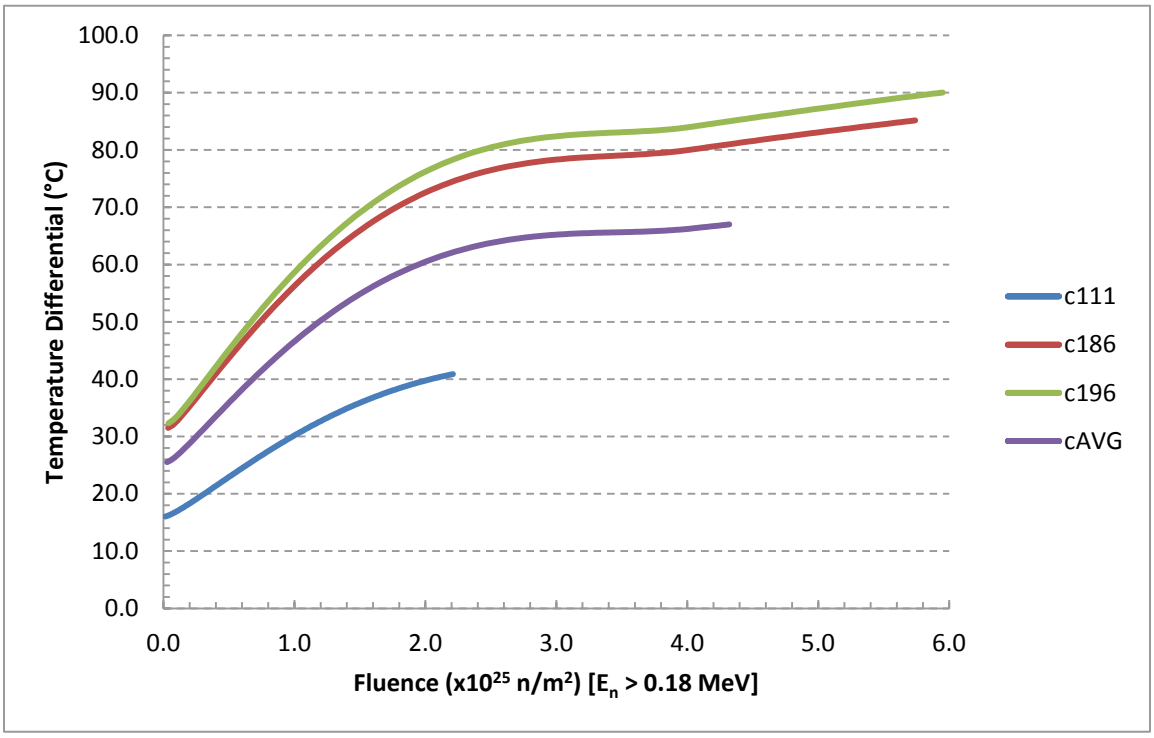

Figure 15. Capsule 1 particle temperature differentials (kernel centerline to outer OPyC).

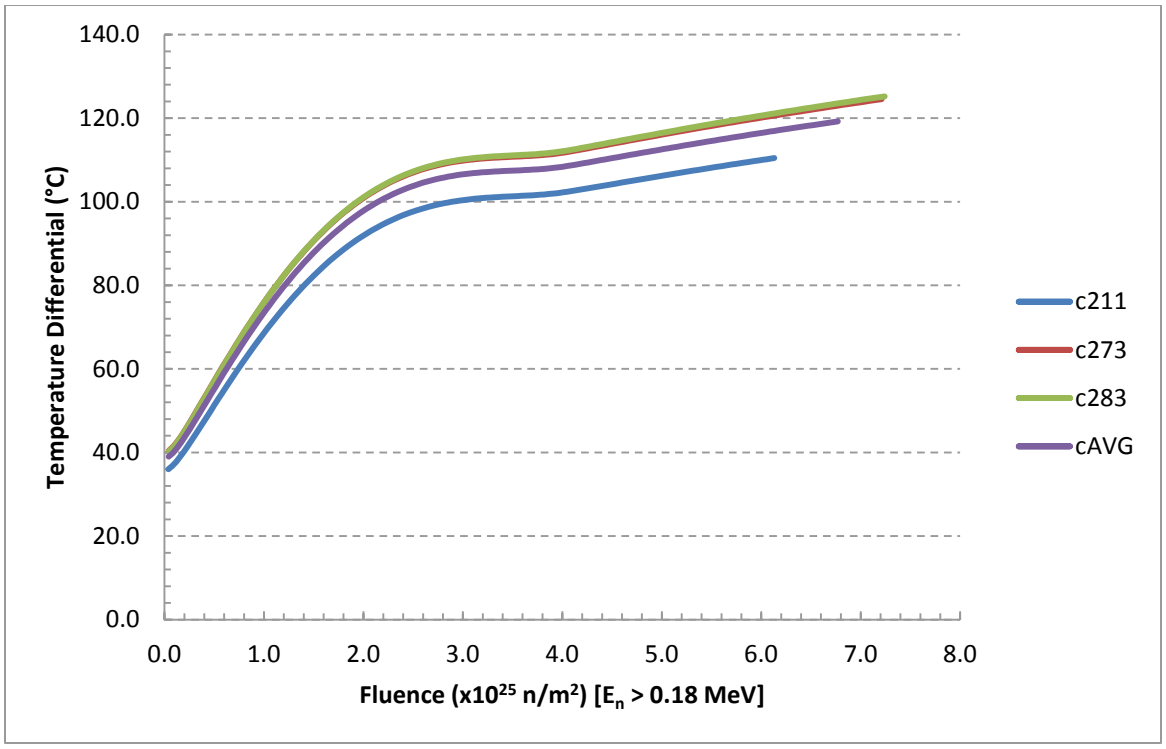

Figure 16. Capsule 2 particle temperature differentials (kernel centerline to outer OPyC).

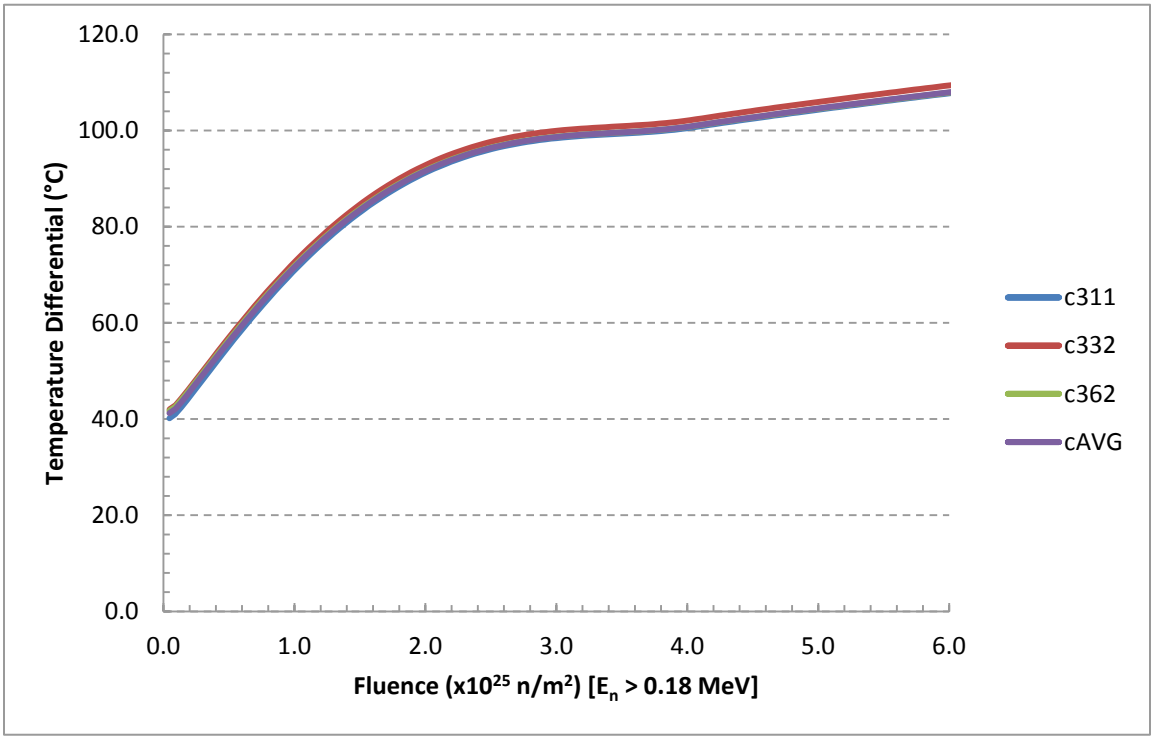

Figure 17. Capsule 3 particle temperature differentials (kernel centerline to outer OPyC).

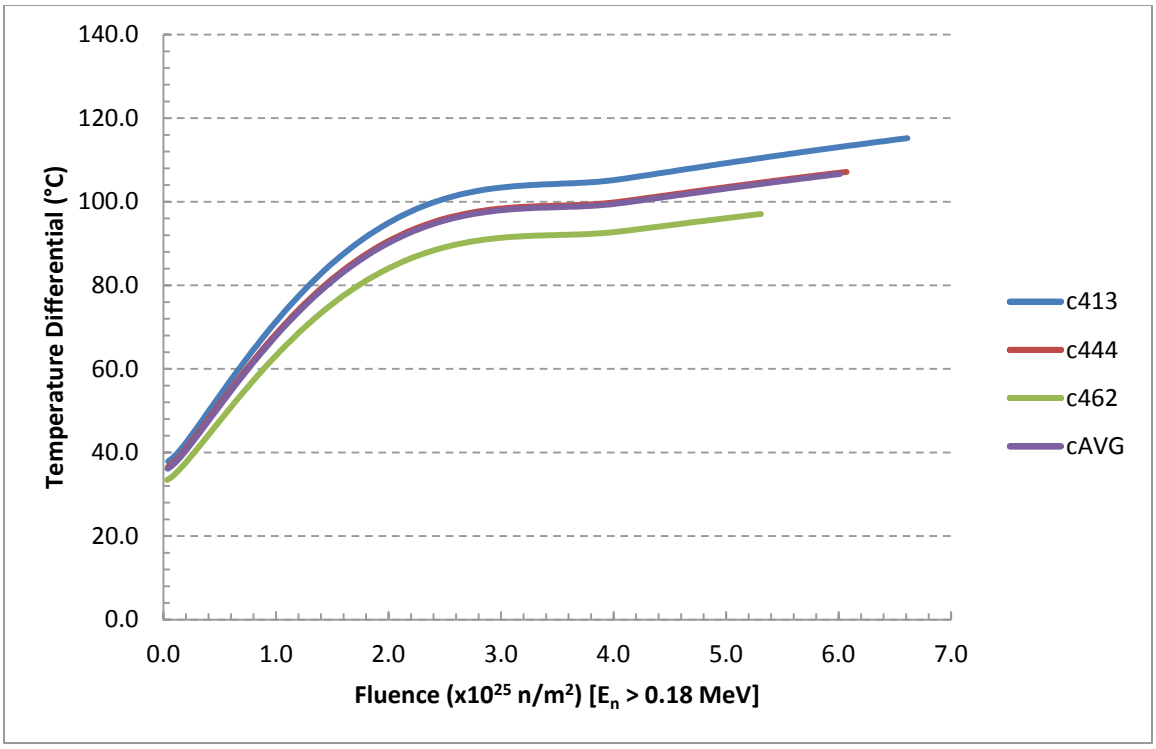

Figure 18. Capsule 4 particle temperature differentials (kernel centerline to outer OPyC).

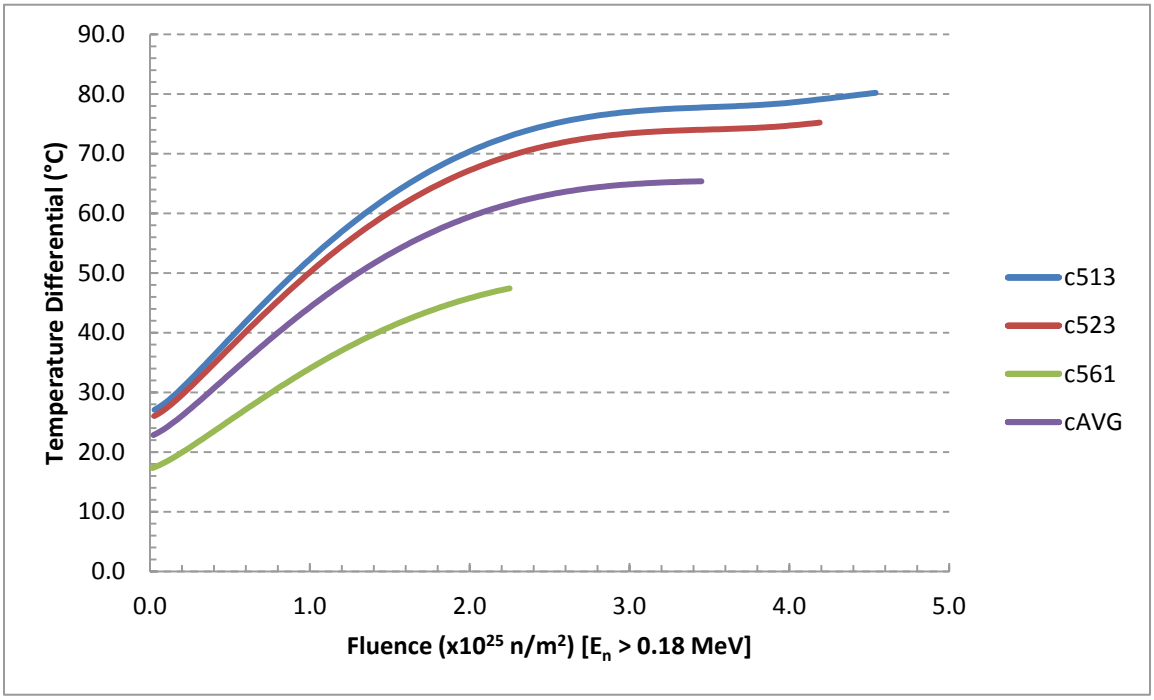

Figure 19. Capsule 5 particle temperature differentials (kernel centerline to outer OPyC).

4.3 Release Fraction

The release fraction (the ratio of the number of atoms released to the number of atoms generated) from the TRISO fuel particles was also analyzed in a separate analysis using the TAVA temperatures of each of the 20 compacts chosen for this study. The predicted irradiation temperatures (Murray 2017) were applied at the outer surface of the OPyC layer. The release from the fuel particles includes uranium contamination (3.18×10^{-5} for Capsules 1 and 5 and 2.66×10^{-5} for Capsules 2 through 4). A summary of the release fraction results can be found in Table 6, with the complete results presented in Appendix A. The results are based on the number of atoms released from 2275 (Capsules 2, 3, and 4) and 3442 (Capsules 1 and 5) fuel particles. The results presented in this analysis can be used as the source term for further fission product diffusion analysis.

Table 6. AGR-5/6/7 average fractional release by particles.

Capsule	Compact	Fluence ($\times 10^{25}$ n/m^2)	Burnup (%FIMA)	TAVA (°C)	Ag	Cs	Sr
1	1-1-1	2.21	7.42	888	7.76E-05	4.46E-05	1.99E-07
	1-8-6	5.74	13.96	1241	3.97E-01	6.97E-03	3.83E-03
	1-9-6	5.95	14.47	1146	1.38E-01	7.59E-04	7.78E-05
	Average	4.32	11.49	1105	6.86E-02	8.15E-05	1.26E-05
2	2-1-1	6.13	16.71	851	9.40E-05	4.40E-05	6.08E-08
	2-7-3	7.21	18.58	935	8.37E-05	2.80E-05	5.42E-07
	2-8-3	7.24	18.56	923	5.05E-05	2.70E-05	4.09E-07
	Average	6.77	17.97	910	3.77E-05	2.58E-05	2.97E-07
3	3-1-1	7.13	17.70	1292	5.64E-01	2.51E-02	2.52E-02
	3-3-2	7.35	18.33	1405	8.26E-01	8.75E-02	1.62E-01
	3-6-2	7.18	18.19	1421	8.48E-01	9.75E-02	1.91E-01
	Average	7.17	18.03	1382	7.88E-01	6.80E-02	1.21E-01
4	4-1-3	6.61	17.44	913	3.94E-05	2.60E-05	3.20E-07
	4-4-4	6.07	16.77	933	7.44E-05	2.77E-05	5.17E-07
	4-6-2	5.31	15.47	881	7.45E-05	4.29E-05	1.40E-07
	Average	6.01	16.63	916	4.15E-05	2.62E-05	3.44E-07
5	5-1-3	4.54	12.67	803	8.48E-05	2.92E-05	1.71E-08
	5-2-3	4.19	12.17	812	9.25E-05	3.31E-05	2.27E-08
	5-6-1	2.25	8.24	696	2.72E-05	5.76E-06	3.79E-10
	Average	3.45	10.74	777	7.35E-05	2.27E-05	7.36E-09

4.4 Release to Birth Ratios

The release to birth (R/B) ratios were calculated for both the dispersed uranium fraction (3.18×10^{-5} for Capsules 1 and 5 and 2.66×10^{-5} for Capsules 2 through 4) and exposed kernel fraction (6.57×10^{-5} for Capsules 1 and 5 and 7.39×10^{-6} for Capsules 2 through 4) to determine the total R/B ratios for 12 isotopes of interest. These results are presented in Appendix B for each minimum, maximum, and average TAVA temperature compact.

5. CONCLUSION

Fuel particle failure analysis was completed using PARFUME to analyze the failure probability of the AGR-5/6/7 irradiation test. The AGR-5/6/7 test consists of irradiating five capsules in the NEFT position of ATR for approximately 500 EFPDs. Using predicted neutronic physics and thermal data, the fuel particle failure probability, buffer-IPyC gap formation, and release from the TRISO fuel particles have been analyzed. The following summarizes the results derived from this work.

Failure probabilities are predicted to be low, resulting in fuel particle failures in compacts only in Capsule 3 and Capsule 5.

The irradiation conditions of the AGR-5/6/7 test result in a prediction of zero fuel particle failures in the compacts in Capsules 1, 2, and 4. Fuel particle failures were predicted in some of the compacts in Capsule 3 due to internal particle pressure. The internal pressure is magnified due to the fuel particles asphericity (1.04). Assuming a perfectly spherical particle, there are no predicted fuel particle failures due to pressure in any compact in Capsule 3. Capsule 5 contained compacts that exhibited fuel particle failures that were due to IPyC cracking, causing localized stress concentrations in the SiC layer. This capsule is to be irradiated at lower temperatures, resulting in a slower creep rate of the pyrocarbon layers, which causes an increase in localized stresses resulting in an increase in the probability of IPyC cracking.

Irradiation-induced shrinkage of the buffer and IPyC layer resulted in the formation of a buffer-IPyC gap.

As expected, shrinkage of the buffer and IPyC layer during irradiation resulted in formation of a buffer-IPyC gap. The two capsules at the two ends of the test train, Capsules 1 and 5, experienced the smallest buffer-IPyC gap formation due to the lower irradiation fluences and temperatures. Capsule 3 experienced the largest buffer-IPyC gap formation of just under 23.9 μm.

The release fraction of fission products varies depending on temperature.

The release fraction of fission products Ag, Cs, and Sr vary depending on capsule location and irradiation temperature. The maximum release fraction of Ag occurs in Capsule 3, reaching up to 84.8% for the TRISO fuel particles. The release fraction of the other two fission products, Cs and Sr, are much smaller and, in most cases, less than 1%. The notable exception is again in Capsule 3, where the release fractions for Cs and Sr reach up to 9.7 and 19.1%, respectively.

The R/B ratios vary by isotope and compact temperature.

Considering both uranium contamination and exposed kernels, the R/B ratios vary by isotope and range from 8.38×10^{-9} to 3.28×10^{-5}. As expected, the compacts that had the highest TAVA temperatures experienced the highest R/B ratios.

6. REFERENCES

Abaqus, 2009, *Abaqus User's Manual*, Dassault Systemes Simulia Corp.

ASME, 2008, NQA-1-2008/-1a-2009, "Quality Assurance Requirements for Nuclear Facility Applications," American Society of Mechanical Engineers, March 2008 (Addenda August 2009).

CEGA, 1993, "NP-MHTGR Material Models of Pyrocarbon and Pyrolytic Silicon Carbide," CEGA-002820, Rev. 1, CEGA Corporation, San Diego, CA, July 1993.

Collin, B.P., 2017, PLN-5245, "AGR-5/6/7 Irradiation Experiment Test Plan," Rev. 0, Idaho National Laboratory, September 7, 2017.

INL, 2017, PLN-3636, "Technical Program Plan for INL Advanced Reactor Technologies Technology Development Office/Advanced Gas Reactor Fuel Development and Qualification Program," Rev. 6, Idaho National Laboratory, June 28, 2017.

Maki, J.T., 2017, SPC-1749, "AGR-5/6/7 Irradiation Test Specification," Rev. 0, Idaho National Laboratory, July 8, 2015.

Marshall, D.W., 2017, SPC-1352, "AGR-5/6/7 Fuel Specification," Rev. 8, Idaho National Laboratory, March 9, 2017.

Miller, G.K., D.A. Petti, D.J. Varacalle Jr., and J.T. Maki, 2003, "Statistical approach and benchmarking for modeling of multi-dimensional behavior in TRISO-coated fuel particles," *Journal of Nuclear Materials*, Volume 317, April 2003, pp. 69–82.

Miller, G.K., D.A. Petti, and J.T. Maki, 2004, "Consideration of the effects of partial debonding of the IPyC and particle asphericity on TRISO-coated fuel behavior," *Journal of Nuclear Materials*, Volume 334, September 2004, pp. 79–89.

Miller, G. K., and D.L. Knudson, 2007, EDF-5741, "Advanced Gas Reactor-1 Pre-Test Prediction Analyses Using the PARFUME Code," Rev. 1, Idaho National Laboratory, April 25, 2007.

Miller, G.K., D.A. Petti, J.T. Maki, and D.L. Knudson, 2009, *PARFUME Theory and Model Basis Report,* INL/EXT-08-14497, Idaho National Laboratory, September 2009.

Murray, P.E., 2017, ECAR-2966, "Thermal Analysis of the AGR-5-6-7 Experiment," Rev. 3, Idaho National Laboratory, April 6, 2017.

Skerjanc, W.F., J.T. Maki, B.P. Collin, and D.A. Petti, 2016, "Evaluation of design parameters for TRISO-coated fuel particles to establish manufacturing critical limits using PARFUME," *Journal of Nuclear Materials*, Volume 469, February 2016, pp. 99–105.

Sterbentz, J.W., 2017, ECAR-2961, "JMOCUP Physics Depletion Calculation for the Design of the AGR-5/6/7 TRISO Particle Experiment in ATR Northeast Flux Trap," Rev. 6, Idaho National Laboratory, June 13, 2017.

Appendix A

Fission Product Release

Table A-1. Summary of inventory (number of atoms) released by the particles.

Capsule	Compact	Fluence ($x10^{25}$ n/m^2)	Burnup (%FIMA)	TAVA (°C)	Ag	Cs	Sr
1	1-1-1	2.21	7.42	888	4.97E+13	1.51E+15	4.52E+12
	1-8-6	5.74	13.96	1241	6.71E+17	4.43E+17	1.44E+17
	1-9-6	5.95	14.47	1146	2.46E+17	5.00E+16	3.01E+15
	Average	4.32	11.49	1105	8.59E+16	4.26E+15	4.07E+14
2	2-1-1	6.13	16.71	851	1.39E+14	2.21E+15	1.74E+12
	2-7-3	7.21	18.58	935	1.45E+14	1.56E+15	1.69E+13
	2-8-3	7.24	18.56	923	8.75E+13	1.51E+15	1.27E+13
	Average	6.77	17.97	910	6.22E+13	1.39E+15	9.03E+12
3	3-1-1	7.13	17.70	1292	9.08E+17	1.33E+18	7.58E+17
	3-3-2	7.35	18.33	1405	1.40E+18	4.83E+18	5.01E+18
	3-6-2	7.18	18.19	1421	1.43E+18	5.33E+18	5.86E+18
	Average	7.17	18.03	1382	1.31E+18	3.69E+18	3.68E+18
4	4-1-3	6.61	17.44	913	6.20E+13	1.36E+15	9.49E+12
	4-4-4	6.07	16.77	933	1.10E+14	1.40E+15	1.49E+13
	4-6-2	5.31	15.47	881	9.75E+13	1.99E+15	3.77E+12
	Average	6.01	16.63	916	6.07E+13	1.31E+15	9.84E+12
5	5-1-3	4.54	12.67	803	1.23E+14	1.68E+15	5.96E+11
	5-2-3	4.19	12.17	812	1.26E+14	1.83E+15	7.64E+11
	5-6-1	2.25	8.24	696	2.04E+13	2.16E+14	9.35E+09
	Average	3.45	10.74	777	8.29E+13	1.11E+15	2.25E+11

Appendix B

Release to Birth (R/B) Ratios

Table B-1. Maximum R/B ratios for Kr-90.

Capsule	Compact	TAVA (°C)	Kr-90			Notes
			Dispersed Uranium	Exposed Kernel	Total	
1	c111	888	1.47E-08	3.02E-08	4.49E-08	Minimum TAVA
	c186	1241	5.29E-08	2.13E-07	2.66E-07	Maximum TAVA
	cAVG	1105	3.49E-08	1.13E-07	1.48E-07	Average TAVA
2	c211	851	1.03E-08	4.18E-09	1.45E-08	Minimum TAVA
	c273	935	1.52E-08	7.35E-09	2.26E-08	Maximum TAVA
	cAVG	910	1.36E-08	6.23E-09	1.99E-08	Average TAVA
3	c311	1292	5.08E-08	3.15E-08	8.22E-08	Minimum TAVA
	c362	1421	6.92E-08	4.71E-08	1.16E-07	Maximum TAVA
	cAVG	1382	6.33E-08	4.20E-08	1.05E-07	Average TAVA
4	c462	881	1.19E-08	4.63E-09	1.65E-08	Minimum TAVA
	c444	933	1.51E-08	6.61E-09	2.17E-08	Maximum TAVA
	cAVG	916	1.40E-08	6.00E-09	2.00E-08	Average TAVA
5	c561	696	4.96E-09	1.86E-08	2.36E-08	Minimum TAVA
	c523	812	1.00E-08	2.44E-08	3.44E-08	Maximum TAVA
	cAVG	777	8.23E-09	2.26E-08	3.08E-08	Average TAVA

Table B-2. Maximum R/B ratios for Kr-89.

Capsule	Compact	TAVA (°C)	Kr-89			Notes
			Dispersed Uranium	Exposed Kernel	Total	
1	c111	888	3.56E-08	7.31E-08	1.09E-07	Minimum TAVA
	c186	1241	1.28E-07	5.16E-07	6.44E-07	Maximum TAVA
	cAVG	1105	8.46E-08	2.75E-07	3.59E-07	Average TAVA
2	c211	851	2.49E-08	1.01E-08	3.50E-08	Minimum TAVA
	c273	935	3.69E-08	1.78E-08	5.47E-08	Maximum TAVA
	cAVG	910	3.30E-08	1.51E-08	4.81E-08	Average TAVA
3	c311	1292	1.23E-07	7.61E-08	1.99E-07	Minimum TAVA
	c362	1421	1.67E-07	1.14E-07	2.81E-07	Maximum TAVA
	cAVG	1382	1.53E-07	1.01E-07	2.55E-07	Average TAVA
4	c462	881	2.88E-08	1.12E-08	4.00E-08	Minimum TAVA
	c444	933	3.66E-08	1.60E-08	5.26E-08	Maximum TAVA
	cAVG	916	3.39E-08	1.45E-08	4.85E-08	Average TAVA
5	c561	696	1.20E-08	4.51E-08	5.71E-08	Minimum TAVA
	c523	812	2.43E-08	5.90E-08	8.33E-08	Maximum TAVA
	cAVG	777	1.99E-08	5.47E-08	7.46E-08	Average TAVA

Table B-3. Maximum R/B ratios for Kr-87.

Capsule	Compact	TAVA (°C)	Kr-87			Notes
			Dispersed Uranium	Exposed Kernel	Total	
1	c111	888	1.75E-07	3.58E-07	5.33E-07	Minimum TAVA
	c186	1241	6.25E-07	2.50E-06	3.13E-06	Maximum TAVA
	cAVG	1105	4.13E-07	1.34E-06	1.75E-06	Average TAVA
2	c211	851	1.22E-07	4.95E-08	1.71E-07	Minimum TAVA
	c273	935	1.81E-07	8.70E-08	2.68E-07	Maximum TAVA
	cAVG	910	1.62E-07	7.38E-08	2.35E-07	Average TAVA
3	c311	1292	5.99E-07	3.68E-07	9.67E-07	Minimum TAVA
	c362	1421	8.14E-07	5.47E-07	1.36E-06	Maximum TAVA
	cAVG	1382	7.46E-07	4.88E-07	1.23E-06	Average TAVA
4	c462	881	1.41E-07	5.49E-08	1.96E-07	Minimum TAVA
	c444	933	1.79E-07	7.83E-08	2.57E-07	Maximum TAVA
	cAVG	916	1.66E-07	7.11E-08	2.37E-07	Average TAVA
5	c561	696	5.89E-08	2.21E-07	2.80E-07	Minimum TAVA
	c523	812	1.19E-07	2.89E-07	4.08E-07	Maximum TAVA
	cAVG	777	9.78E-08	2.68E-07	3.66E-07	Average TAVA

Table B-4. Maximum R/B ratios for Kr-88.

Capsule	Compact	TAVA (°C)	Kr-88			Notes
			Dispersed Uranium	Exposed Kernel	Total	
1	c111	888	2.61E-07	5.36E-07	7.97E-07	Minimum TAVA
	c186	1241	9.32E-07	3.72E-06	4.66E-06	Maximum TAVA
	cAVG	1105	6.17E-07	2.00E-06	2.62E-06	Average TAVA
2	c211	851	1.82E-07	7.41E-08	2.56E-07	Minimum TAVA
	c273	935	2.70E-07	1.30E-07	4.00E-07	Maximum TAVA
	cAVG	910	2.42E-07	1.10E-07	3.52E-07	Average TAVA
3	c311	1292	8.93E-07	5.47E-07	1.44E-06	Minimum TAVA
	c362	1421	1.21E-06	8.08E-07	2.02E-06	Maximum TAVA
	cAVG	1382	1.11E-06	7.23E-07	1.83E-06	Average TAVA
4	c462	881	2.11E-07	8.20E-08	2.93E-07	Minimum TAVA
	c444	933	2.68E-07	1.17E-07	3.85E-07	Maximum TAVA
	cAVG	916	2.48E-07	1.06E-07	3.55E-07	Average TAVA
5	c561	696	8.81E-08	3.31E-07	4.19E-07	Minimum TAVA
	c523	812	1.78E-07	4.33E-07	6.11E-07	Maximum TAVA
	cAVG	777	1.46E-07	4.01E-07	5.47E-07	Average TAVA

Table B-5. Maximum R/B ratios for Kr-85m.

Capsule	Compact	TAVA (°C)	Kr-85m			Notes
			Dispersed Uranium	Exposed Kernel	Total	
1	c111	888	3.28E-07	6.72E-07	1.00E-06	Minimum TAVA
	c186	1241	1.17E-06	4.65E-06	5.82E-06	Maximum TAVA
	cAVG	1105	7.74E-07	2.50E-06	3.28E-06	Average TAVA
2	c211	851	2.29E-07	9.30E-08	3.22E-07	Minimum TAVA
	c273	935	3.39E-07	1.63E-07	5.02E-07	Maximum TAVA
	cAVG	910	3.03E-07	1.38E-07	4.42E-07	Average TAVA
3	c311	1292	1.12E-06	6.82E-07	1.80E-06	Minimum TAVA
	c362	1421	1.52E-06	1.00E-06	2.52E-06	Maximum TAVA
	cAVG	1382	1.39E-06	9.00E-07	2.29E-06	Average TAVA
4	c462	881	2.65E-07	1.03E-07	3.68E-07	Minimum TAVA
	c444	933	3.36E-07	1.47E-07	4.83E-07	Maximum TAVA
	cAVG	916	3.12E-07	1.33E-07	4.45E-07	Average TAVA
5	c561	696	1.11E-07	4.15E-07	5.26E-07	Minimum TAVA
	c523	812	2.23E-07	5.43E-07	7.67E-07	Maximum TAVA
	cAVG	777	1.84E-07	5.03E-07	6.87E-07	Average TAVA

Table B-6. Maximum R/B ratios for Xe-139.

Capsule	Compact	TAVA (°C)	Xe-139			Notes
			Dispersed Uranium	Exposed Kernel	Total	
1	c111	888	5.10E-09	3.36E-08	3.87E-08	Minimum TAVA
	c186	1241	1.32E-08	2.37E-07	2.50E-07	Maximum TAVA
	cAVG	1105	9.67E-09	1.26E-07	1.36E-07	Average TAVA
2	c211	851	3.73E-09	4.65E-09	8.38E-09	Minimum TAVA
	c273	935	4.99E-09	8.17E-09	1.32E-08	Maximum TAVA
	cAVG	910	4.60E-09	6.93E-09	1.15E-08	Average TAVA
3	c311	1292	1.22E-08	3.50E-08	4.72E-08	Minimum TAVA
	c362	1421	1.53E-08	5.24E-08	6.78E-08	Maximum TAVA
	cAVG	1382	1.44E-08	4.67E-08	6.11E-08	Average TAVA
4	c462	881	4.16E-09	5.15E-09	9.31E-09	Minimum TAVA
	c444	933	4.96E-09	7.36E-09	1.23E-08	Maximum TAVA
	cAVG	916	4.69E-09	6.68E-09	1.14E-08	Average TAVA
5	c561	696	2.27E-09	2.07E-08	2.30E-08	Minimum TAVA
	c523	812	3.83E-09	2.71E-08	3.10E-08	Maximum TAVA
	cAVG	777	3.31E-09	2.51E-08	2.84E-08	Average TAVA

Table B-7. Maximum R/B ratios for Xe-137.

Capsule	Compact	TAVA (°C)	Xe-137			Notes
			Dispersed Uranium	Exposed Kernel	Total	
1	c111	888	1.22E-08	8.06E-08	9.28E-08	Minimum TAVA
	c186	1241	3.16E-08	5.69E-07	6.00E-07	Maximum TAVA
	cAVG	1105	2.32E-08	3.03E-07	3.26E-07	Average TAVA
2	c211	851	8.95E-09	1.12E-08	2.01E-08	Minimum TAVA
	c273	935	1.20E-08	1.96E-08	3.16E-08	Maximum TAVA
	cAVG	910	1.10E-08	1.66E-08	2.77E-08	Average TAVA
3	c311	1292	2.93E-08	8.39E-08	1.13E-07	Minimum TAVA
	c362	1421	3.68E-08	1.25E-07	1.62E-07	Maximum TAVA
	cAVG	1382	3.45E-08	1.12E-07	1.46E-07	Average TAVA
4	c462	881	9.98E-09	1.24E-08	2.23E-08	Minimum TAVA
	c444	933	1.19E-08	1.77E-08	2.96E-08	Maximum TAVA
	cAVG	916	1.13E-08	1.60E-08	2.73E-08	Average TAVA
5	c561	696	5.46E-09	4.97E-08	5.52E-08	Minimum TAVA
	c523	812	9.20E-09	6.51E-08	7.43E-08	Maximum TAVA
	cAVG	777	7.95E-09	6.03E-08	6.83E-08	Average TAVA

Table B-8. Maximum R/B ratios for Xe-138.

Capsule	Compact	TAVA (°C)	Xe-138			Notes
			Dispersed Uranium	Exposed Kernel	Total	
1	c111	888	2.34E-08	1.54E-07	1.78E-07	Minimum TAVA
	c186	1241	6.05E-08	1.09E-06	1.15E-06	Maximum TAVA
	cAVG	1105	4.45E-08	5.79E-07	6.24E-07	Average TAVA
2	c211	851	1.71E-08	2.14E-08	3.85E-08	Minimum TAVA
	c273	935	2.30E-08	3.75E-08	6.05E-08	Maximum TAVA
	cAVG	910	2.11E-08	3.18E-08	5.30E-08	Average TAVA
3	c311	1292	5.60E-08	1.60E-07	2.16E-07	Minimum TAVA
	c362	1421	7.05E-08	2.39E-07	3.09E-07	Maximum TAVA
	cAVG	1382	6.60E-08	2.13E-07	2.79E-07	Average TAVA
4	c462	881	1.91E-08	2.37E-08	4.28E-08	Minimum TAVA
	c444	933	2.28E-08	3.38E-08	5.66E-08	Maximum TAVA
	cAVG	916	2.16E-08	3.07E-08	5.23E-08	Average TAVA
5	c561	696	1.05E-08	9.53E-08	1.06E-07	Minimum TAVA
	c523	812	1.76E-08	1.25E-07	1.42E-07	Maximum TAVA
	cAVG	777	1.52E-08	1.16E-07	1.31E-07	Average TAVA

Table B-9. Maximum R/B ratios for Xe-135m.

Capsule	Compact	TAVA (°C)	Xe-135m			Notes
			Dispersed Uranium	Exposed Kernel	Total	
1	c111	888	2.44E-08	1.61E-07	1.85E-07	Minimum TAVA
	c186	1241	6.30E-08	1.13E-06	1.19E-06	Maximum TAVA
	cAVG	1105	4.63E-08	6.03E-07	6.50E-07	Average TAVA
2	c211	851	1.79E-08	2.23E-08	4.01E-08	Minimum TAVA
	c273	935	2.39E-08	3.91E-08	6.30E-08	Maximum TAVA
	cAVG	910	2.20E-08	3.32E-08	5.52E-08	Average TAVA
3	c311	1292	5.84E-08	1.67E-07	2.25E-07	Minimum TAVA
	c362	1421	7.35E-08	2.49E-07	3.22E-07	Maximum TAVA
	cAVG	1382	6.88E-08	2.22E-07	2.91E-07	Average TAVA
4	c462	881	1.99E-08	2.46E-08	4.46E-08	Minimum TAVA
	c444	933	2.38E-08	3.52E-08	5.90E-08	Maximum TAVA
	cAVG	916	2.25E-08	3.20E-08	5.44E-08	Average TAVA
5	c561	696	1.09E-08	9.92E-08	1.10E-07	Minimum TAVA
	c523	812	1.84E-08	1.30E-07	1.48E-07	Maximum TAVA
	cAVG	777	1.59E-08	1.20E-07	1.36E-07	Average TAVA

Table B-10. Maximum R/B ratios for Xe-135.

Capsule	Compact	TAVA (°C)	Xe-135			Notes
			Dispersed Uranium	Exposed Kernel	Total	
1	c111	888	1.46E-07	9.57E-07	1.10E-06	Minimum TAVA
	c186	1241	3.75E-07	6.56E-06	6.94E-06	Maximum TAVA
	cAVG	1105	2.76E-07	3.55E-06	3.83E-06	Average TAVA
2	c211	851	1.07E-07	1.32E-07	2.39E-07	Minimum TAVA
	c273	935	1.43E-07	2.32E-07	3.74E-07	Maximum TAVA
	cAVG	910	1.31E-07	1.97E-07	3.28E-07	Average TAVA
3	c311	1292	3.47E-07	9.58E-07	1.31E-06	Minimum TAVA
	c362	1421	4.37E-07	1.40E-06	1.84E-06	Maximum TAVA
	cAVG	1382	4.09E-07	1.26E-06	1.67E-06	Average TAVA
4	c462	881	1.19E-07	1.46E-07	2.65E-07	Minimum TAVA
	c444	933	1.42E-07	2.09E-07	3.50E-07	Maximum TAVA
	cAVG	916	1.34E-07	1.90E-07	3.24E-07	Average TAVA
5	c561	696	6.50E-08	5.91E-07	6.56E-07	Minimum TAVA
	c523	812	1.10E-07	7.73E-07	8.83E-07	Maximum TAVA
	cAVG	777	9.47E-08	7.17E-07	8.11E-07	Average TAVA

Table B-11. Maximum R/B ratios for Xe-133.

Capsule	Compact	TAVA (°C)	Xe-133			Notes
			Dispersed Uranium	Exposed Kernel	Total	
1	c111	888	5.40E-07	3.51E-06	4.05E-06	Minimum TAVA
	c186	1241	1.38E-06	2.21E-05	2.34E-05	Maximum TAVA
	cAVG	1105	1.02E-06	1.25E-05	1.36E-05	Average TAVA
2	c211	851	3.95E-07	4.84E-07	8.79E-07	Minimum TAVA
	c273	935	5.28E-07	8.37E-07	1.37E-06	Maximum TAVA
	cAVG	910	4.87E-07	7.14E-07	1.20E-06	Average TAVA
3	c311	1292	1.28E-06	3.11E-06	4.38E-06	Minimum TAVA
	c362	1421	1.60E-06	4.19E-06	5.79E-06	Maximum TAVA
	cAVG	1382	1.50E-06	3.87E-06	5.37E-06	Average TAVA
4	c462	881	4.40E-07	5.35E-07	9.75E-07	Minimum TAVA
	c444	933	5.25E-07	7.56E-07	1.28E-06	Maximum TAVA
	cAVG	916	4.97E-07	6.89E-07	1.19E-06	Average TAVA
5	c561	696	2.42E-07	2.18E-06	2.42E-06	Minimum TAVA
	c523	812	4.06E-07	2.85E-06	3.25E-06	Maximum TAVA
	cAVG	777	3.52E-07	2.64E-06	2.99E-06	Average TAVA

Table B-12. Maximum R/B ratios for Xe-131m.

Capsule	Compact	TAVA (°C)	Xe-131m			Notes
			Dispersed Uranium	Exposed Kernel	Total	
1	c111	888	8.11E-07	5.24E-06	6.05E-06	Minimum TAVA
	c186	1241	2.07E-06	3.08E-05	3.28E-05	Maximum TAVA
	cAVG	1105	1.53E-06	1.82E-05	1.97E-05	Average TAVA
2	c211	851	5.94E-07	7.21E-07	1.31E-06	Minimum TAVA
	c273	935	7.93E-07	1.23E-06	2.03E-06	Maximum TAVA
	cAVG	910	7.31E-07	1.06E-06	1.79E-06	Average TAVA
3	c311	1292	1.91E-06	4.20E-06	6.11E-06	Minimum TAVA
	c362	1421	2.39E-06	5.31E-06	7.70E-06	Maximum TAVA
	cAVG	1382	2.24E-06	5.01E-06	7.25E-06	Average TAVA
4	c462	881	6.62E-07	7.96E-07	1.46E-06	Minimum TAVA
	c444	933	7.88E-07	1.12E-06	1.91E-06	Maximum TAVA
	cAVG	916	7.46E-07	1.02E-06	1.77E-06	Average TAVA
5	c561	696	3.64E-07	3.27E-06	3.63E-06	Minimum TAVA
	c523	812	6.11E-07	4.26E-06	4.87E-06	Maximum TAVA
	cAVG	777	5.29E-07	3.95E-06	4.48E-06	Average TAVA